UNIVERSITY OF COPENHAGEN
FACULTY OF SCIENCE

Master Thesis

Johannes Fuglseth Bæk

Black Hole Merger in Active Galactic Nuclei environment through 3-body interactions

Date: August 11, 2023

Supervisor: Johan Samsing

Abstract

Black hole mergers is an active area of research in astrophysics with multiple viable channels. Their merger through gravitational radiation with no interference would entail a merger time greater than a Hubble time and which data from LIGO contradicts. Many mechanisms have been proposed to explain this discrepancy one of which is that binary black holes could have their orbits significantly modified by the interference of a third black hole. Building on the work done by D'Orazio and Samsing, and their merger probabilities for isolated 3-body systems, the environment of a super massive black hole around which the 3 bodies orbited was added in order to determine the merger probability as a function of distance to the super massive black hole. The theoretical framework was worked out from the isolated 3-body system energy distribution and verified by numerical results taken from 10^4 simulations for a select distance to the super massive black hole. From this the theoretical distribution seemed to be verified and showed that the merger probability decreases along with the distance to the super massive black hole while quickly approaching the isolated distribution as the 3-body system is moved away from the super massive black hole. While this is still a simplified model it does seem to support the 3-body interactions as a viable source for gravitational waves.

Acknowledgement

I would like to thank my supervisor Johan Samsing and Daniel D'Orazio for guidance and advice during the project, as well as Martin Pessah for help in preparation for the project. I would also like to thank my friends and family for help and support during the writing for this project.

Contents

1 Introduction **1**

2 General Relativity **4**
2.1 Equations of motion in General Relativity 5
2.2 Weak Gravitational Field limit 6
2.3 Einstein field equation 7
2.4 Gravitational waves 9
2.4.1 Binary GW radiation 10
2.5 Post-Newtonian Expansion 13

3 Stellar Evolution **15**
3.1 Separate Evolution 15
3.2 Common Evolution 15
3.2.1 Common Envelope Channel 16
3.2.2 Chemically-Homogenous Evolution Channel 17
3.3 Dynamical Evolution 18
3.4 3-Body interactions 19
3.5 Derivation of merger probabilities 22
3.6 Super Massive Black Holes 25
3.6.1 Newtonian potential 25
3.6.2 Tidal Disruption and regions of gravitational dominance . 26
3.6.3 SMBH probability derivation 26
3.7 Numerical considerations 32
3.7.1 Initial conditions 32
3.7.2 Termination conditions 34

4 Result **36**
4.1 Simulations 36
4.1.1 2-Body simulations 36
4.1.2 3-Body simulations 38
4.1.3 SMBH integration 43

5 Discussion **46**

6 Conclusion **46**

A Code **48**

1 Introduction

In 1916 Albert Einsteins theory of General Relativity predicted the existence of gravitational waves, ripples in space time propagating at the speed of light due to the acceleration of suitably massive objects. The first gravitational wave was detected in 2015 by LIGO (Laser Interferometer Gravitational-Wave Observatory) when they observed what became known as GW150914, a Binary Black Hole (BBH) with masses of roughly $36M_\odot$ and $29M_\odot$ respectively undergoing a merger. This was a huge revelation to the scientific community as it proved that a BBH merger could occur within a Hubble time $t_H = 14.4$ GYr.

This is because naively it is assumed that BBHs must come from a massive Binary Star system undergoing stellar evolution, which involves the expansion into a red giant becoming up to 200 times its initial radius, and subsequent type II Super Nova, both of which would destroy a tightly bound binary. It can however be shown that for a BBH, the vacuum solution for their inspiral and merger is given as[1]:

$$t_{\text{inspiral}} \approx \frac{5}{256} \frac{c^5}{G^3 \mu M^2} a_0^4 \tag{1}$$

with c the speed of light, G the gravitational constant, $\mu = m^2/M$ the reduced mass and $M = m_1 m_2 = m^2$ the system mass assuming equal mass binary. From this we can see that for a merger of stellar mass BBH ($m = 10M_\odot$) to occur within t_H due to gravitational wave radiation, must necessitate their separation to be $a_0 \approx 0.09$AU which is well within the distance of stellar merger as any one of the binaries becomes a red giant.

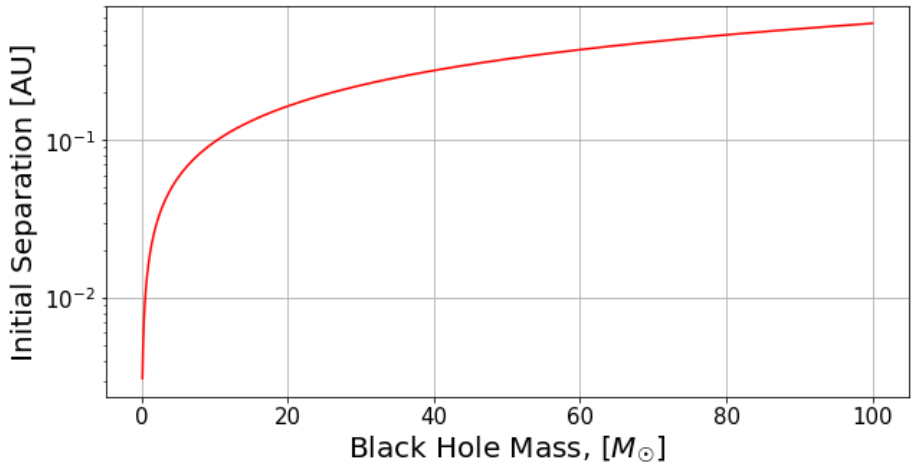

Figure 1: Initial Separation of a BHB as a function of its mass in order for the binary to merge within a Hubble time t_H.

Subsequent BBH mergers were detected in 2016 (GW151226) and seven more

between November 2016 and August 2017 making it abundantly clear that GW150914 was no anomaly and would have to be explained through alternative mechanisms than the naive stellar evolution model. Many papers have been published to explain this paradox with many potential channels for BBH mergers proposed.

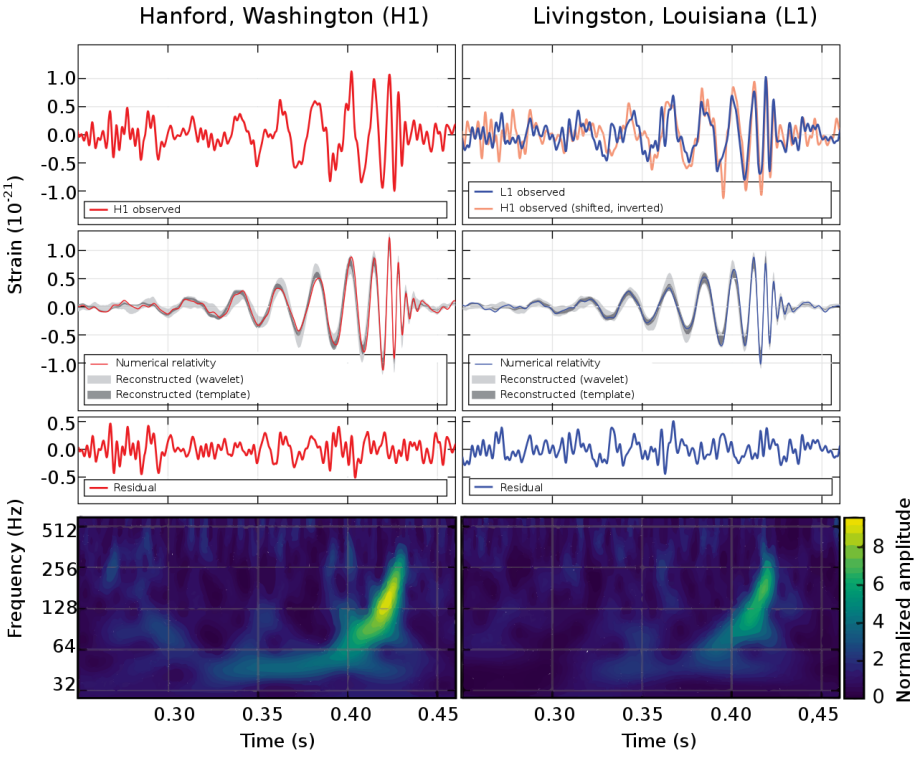

Figure 2: The first observation of gravitational waves observed by LIGO-Virgo in 2016. Known as GW150914, this event matched the predictions for General Relativity and was the result of a black hole merger.

This was especially important when GW190521 was observed. This was the resulting merger of two Black holes with calculated masses being 85 and 66 solar masses. These were the first clear evidence of Intermediate Mass Black Holes, that is, their masses were too great to be formed by the collapse of a single star, meaning they must have acquired mass from their environment, either through earlier mergers or through accretion. The environment needed could be that found in the center of galaxies, known as Active Galactic Nuclei (AGN), where many stellar and intermediate mass black holes could be located in the gravitational environment of a Super-Massive Black Holes (SMBH), absorbing mass from the accretion disk surrounding the SMBH and potentially increasing the number of black hole mergers expected due to the concentration of smaller

black holes[12].

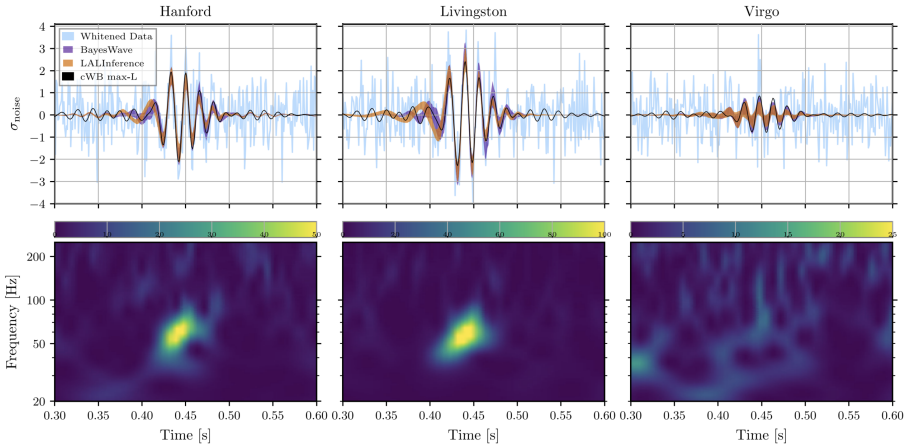

Figure 3: The gravitational waves observed from the merger GW190521, the first evidence for intermediate mass black holes, opening up the possibility for AGN disks as a potential source for Black hole mergers due to the high concentration of black holes and the gas disk of the SMBH, enabling the black holes to increase in mass without the need to merger.

This thesis will explore one of these proposed solutions to the BBH merger paradox. Instead of assuming the BBH merger occurring in isolation, one should take the environment into account. BBHs formed near Galactic nuclei, orbiting SMBH would be unable to go through their merger in isolation, as many other BBHs and single black holes would be located there as well and would distort the Binary's orbit by passing at suitable distances. More intriguing is the possibility that through these single BHs one could imagine a direct encounter in which the binary and the singlet would interact as a 3 body-system, chaotically interacting and greatly distorting the resulting binary's orbital separation and eccentricity. This 3-body interaction has already been explored by Samsing and D'orazio [8][3] but has not taken the greater environment of the SMBH into account. The impact the SMBH, modelled as a simple Newtonian Potential Source, would have on the merger rate of the 3 body system is the focus of this thesis.

2 General Relativity

We begin with the assertions of Einstein that no information can be transmitted faster than the speed of light c, and that as a result our classical notion of space and time are erroneous when moving at speeds $v \approx c$. The entire field of special relativity follows with the main conclusions involving:

- Space and Time are not distinct entities, but are all part of a unified space-time $x = (ct, x, y, z)$
- Every inertial system is equivalent and one can transform from one to another through translation, rotation, and boost.
- The laws of physics does not change when moving from one inertial system to another.

The last point is of course a simplification. In truth this is only the case in-so-far as the physics in question can be expressed *covariantly*, that is to say, it is a frame independent geometric relationship of frame independent geometric objects. In special relativity this geometry in question is flat space time, called Minkowski-Space.
The objects in question must also be covariant. We define the proper time $d\tau$ and proper distance ds between two events at x^μ and $x^\mu + dx^\mu$ as:

$$ds^2 = g_{\mu\nu} dx^\mu dx^\nu = -d\tau^2$$

Where $g_{\mu\nu}$ is the metric which carries the geometric information of the Space-time in question. We see that the proper distance between these two events can have three different values:

- $ds^2 > 0$: space-like separated events
- $ds^2 < 0$: time-like separated events
- $ds^2 = 0$: null separated events

Space-like separated events are causally disconnected since one can find a coordinate system in which these events would happen simultaneously $\Delta x^0 = 0$, which would mean any connection would have to travel faster than light which is impossible. Time-like separated events can be causally connected as one can find a coordinate system where the two events happen at the same spatial point $\Delta x^i = 0$. Null-like separated events can likewise be causally connected but what is special here is that one can only reach from one to the other if one travels at the speed of light.

In Minkowski space the metric $g_{\mu\nu} = \eta_{\mu\nu}$ for cartesian coordinates is given as:

$$\eta = \begin{pmatrix} -1 & 0 & 0 & 0 \\ 0 & 1 & 0 & 0 \\ 0 & 0 & 1 & 0 \\ 0 & 0 & 0 & 1 \end{pmatrix}$$

Special relativity, however, does not account for gravity. There are a lot of different metrics to account for different gravitational environments and we shall not go into specifics here. We will for the most part simply use the generic metric $g_{\mu\nu}$.

Suppose we wished to compute the proper time between two Time-like separated events. We can parametrize the path travelled by some parameter λ. For an infinitisimal element of the the time-like curve we need to travel $x^\mu(\lambda) \to x^\mu(\lambda + d\lambda)$, we can express the proper time as:

$$d\tau^2 = -g_{\mu\nu}dx^\mu dx^\nu = -g_{\mu\nu}\frac{dx^\mu}{d\lambda}\frac{dx^\nu}{d\lambda}d\lambda^2$$

Which by integration gives us the proper time for the whole curve:

$$\Delta\tau = \int_{\lambda_1}^{\lambda_2} d\lambda \sqrt{-g_{\mu\nu}\frac{dx^\mu}{d\lambda}\frac{dx^\nu}{d\lambda}}$$

In Minkowski-Space the un-accelerated path is the path that maximises proper time. A freely falling particle will follow such a path. In General Relativity we call such a path a *Geodesic*.

2.1 Equations of motion in General Relativity

Given the time-like curve $x^\mu(\lambda)$ with proper time:

$$\Delta\tau = \int_{\lambda_1}^{\lambda_2} d\lambda \sqrt{-g_{\mu\nu}\frac{dx^\mu}{d\lambda}\frac{dx^\nu}{d\lambda}}$$

Consider the time-like curve $x^\mu(\lambda) + \delta x^\mu(\lambda)$ that lies infinitesimally close to our original curve and matches the end points $\delta x^\mu(\lambda_1) = \delta x^\mu(\lambda_2) = 0$. Computing the difference in proper time:

$$\delta\Delta\tau = \Delta\tau[x^\mu(\lambda) + \delta x^\mu(\lambda)] - \Delta\tau[x^\mu(\lambda)] \tag{2}$$

For a geodesic $x^\mu(\lambda)$ maximises proper time and as such any curve lying infinitesimally close must have $\delta\Delta\tau = 0$ to first order in $\delta x^\mu(\lambda)$. It can be shown that this gives:

$$\delta\Delta\tau = \int_{\lambda_1}^{\lambda_2} d\tau \left[\frac{d^2x^\mu}{d\tau^2} + \Gamma^\mu_{\nu\rho}\frac{dx^\nu}{d\tau}\frac{dx^\rho}{d\tau}\right] g_{\mu\alpha}\delta x^\alpha = 0$$

Where $\Gamma^\mu_{\nu\rho} = \frac{1}{2}g^{\mu\sigma}\left(\partial_\rho g_{\nu\sigma} + \partial_\nu g_{\rho\sigma} - \partial_\sigma g_{\nu\rho}\right)$ is the Christoffel symbol. Since $\delta\Delta\tau$ should be 0 for any infinitesimal variation δx^α we must have:

$$\frac{d^2x^\mu}{d\tau^2} + \Gamma^\mu_{\nu\rho}\frac{dx^\nu}{d\tau}\frac{dx^\rho}{d\tau} = 0$$

This equation for the motion of freely falling particles as a function of proper time will become important later when extrapolating the acceleration in the Post-Newtonian formalism.

2.2 Weak Gravitational Field limit

In the regime of weak gravitational field we can consider the metric of space time to be a perturbation of the Minkowski metric of the form:

$$g_{\mu\nu}(x) = \eta_{\mu\nu} + h_{\mu\nu}(x)$$

for which all components of the perturbation obeys $|h_{\mu\nu}| \ll 1$ as well as the Lorentz gauge equation:

$$\partial^{\mu}\left(h_{\mu\nu} - \frac{1}{2}\eta_{\mu\nu}\eta^{\rho\sigma}h_{\rho\sigma}\right) = 0$$

Furthermore we demand that our metric be independent of time:

$$\partial_0 g^{\mu\nu} = 0$$

In this limit we also have small velocities:

$$\left|\frac{dx^i}{d\tau}\right| \ll 1$$

The geodesic equation for a freely falling particle in this limit to leading order reads:

$$\frac{d^2x^{\mu}}{d\tau^2} + \Gamma^{\mu}_{00}\left(\frac{dx^0}{d\tau}\right) = 0$$

We can see that to leading order we have:

$$\Gamma^{\mu}_{00} = -\frac{1}{2}\eta^{\mu\sigma}\partial_{\sigma}h_{00}$$

And for $\mu = 0$ we see that $\Gamma^0_{00} = 0$ which means that:

$$\left[\frac{d^2x^{\mu}}{d\tau^2} + \Gamma^{\mu}_{00}\left(\frac{dt}{d\tau}\right)^2\right]_{\mu=0} = \frac{d^2t}{d\tau^2} = 0$$

which means that $dt/d\tau$ must be a constant. We can thus write:

$$\frac{d^2x^i}{dt^2} = \left(\frac{d\tau}{dt}\right)^2\frac{d^2x^i}{d\tau} = -\Gamma^i_{00} = \frac{1}{2}\partial^i h_{00}$$

Comparing this to the newtonian equation which is:

$$\frac{d^2x}{dt^2} = -\overline{\nabla}\phi$$

leading to:

$$-2\phi = h_{00}$$

The weak field limit, and this result will be used in the following sections.

2.3 Einstein field equation

We seek to obtain an analogous equation to the Poisson equations for Newtonian gravity:

$$\nabla^2\phi = 4\pi G\rho$$

with ϕ being the gravitational potential, G the gravitational constant, and ρ the mass density. We know now that the analogue to ϕ would be the metric and thus our new equation should have a left hand side involving the second derivatives of $g_{\mu\nu}(x)$.

Let us define the Riemann curvature tensor:

$$R^{\rho}_{\sigma\mu\nu} = \partial_\mu\Gamma^{\rho}_{\nu\rho} - \partial_\nu\Gamma^{\rho}_{\mu\sigma} + \Gamma^{\rho}_{\alpha\mu}\Gamma^{\alpha}_{\nu\sigma} - \Gamma^{\rho}_{\alpha\nu}\Gamma^{\alpha}_{\mu\sigma}$$

With the following symmetries:

$$\begin{aligned} R_{\mu\nu\rho\sigma} &= -R_{\mu\nu\sigma\rho} = -R_{\nu\mu\rho\sigma} \\ R_{\mu\nu\rho\sigma} &= R_{\sigma\nu\rho\mu} \\ R_{\mu\nu\rho\sigma} + R_{\mu\rho\sigma\nu} + R_{\mu\sigma\nu\rho} &= 0 \end{aligned}$$

Where $R_{\mu\nu\rho\sigma} = g_{\mu\alpha}R^{\alpha}_{\nu\rho\sigma}$. We note here that the Riemann Curvature Tensor obeys the Bianchi-identity.

$$D_\alpha R_{\mu\nu\rho\sigma} + D_\nu R_{\alpha\mu\rho\sigma} + D_\mu R_{\nu\alpha\rho\sigma} = 0$$

From here we define the Ricci tensor

$$R_{\mu\nu} = R^{\rho}_{\mu\rho\nu}$$

We notice here that the Ricci tensor is symmetrical $R_{\mu\nu} = R_{\nu\mu}$ from this we can define the Ricci scalar as the trace of the Ricci tensor

$$R = g^{\mu\nu}R_{\mu\nu}$$

Since both the Ricci tensor and scalar contains the second derivative of the metric we can construct a general second derivative tensor from a linear combination of the Ricci tensor and the product $g_{\mu\nu}R$ of the metric and the Ricci scalar. Our general left hand side thus reads:

$$R_{\mu\nu} + A_c g_{\mu\nu}R$$

Where we set the linear constant of the ricci tensor to 1 for simplicity.

The right hand side must carry some quantitative measure of the energy of the system in question. For this we define the Energy Momentum tensor $T^{\mu\nu}$:

T^{00}	energy density
T^{i0}	density of x^i-component of the momentum
$T^{0,j}$	Energy flux through the surface perpendicular to x^j
T^{ij}	internal forces per unit area dA

This tensor is symmetric $T^{\mu\nu} = T^{\nu\mu}$ and is conserved under the covariant derivative:

$$D_\mu T^{\mu\nu} = 0$$

We now know that the equation must be of the form:

$$R_{\mu\nu} + A_c g_{\mu\nu} R = B_c T_{\mu\nu}$$

with our two constants still undetermined. Since The right hand side must be conserved we can write:

$$D^\mu (R_{\mu\nu} + A_c g_{\mu\nu} R) = 0$$

Here we can utilise the Bianchi identity. We write:

$$\begin{aligned}
D_\alpha R_{\mu\nu\rho\sigma} + D_\nu R_{\alpha\mu\rho\sigma} + D_\mu R_{\nu\alpha\rho\sigma} &= 0 \\
g^{\mu\rho} g^{\nu\sigma} (D_\alpha R_{\mu\nu\rho\sigma} - D_\nu R_{\mu\alpha\rho\sigma} - D_\mu R_{\nu\alpha\sigma\rho}) &= 0 \\
D_\alpha g^{\mu\rho} g^{\nu\sigma} R_{\mu\nu\rho\sigma} - D_\nu g^{\mu\rho} g^{\nu\sigma} R_{\mu\alpha\rho\sigma} - D_\mu g^{\mu\rho} g^{\nu\sigma} R_{\nu\alpha\sigma\rho} &= 0 \\
D_\alpha g^{\nu\sigma} R^\rho_{\nu\rho\sigma} - D_\nu g^{\nu\sigma} R^\rho_{\alpha\rho\sigma} - D_\mu g^{\mu\rho} R^\sigma_{\alpha\sigma\rho} &= 0 \\
D_\alpha R - 2 D^\beta R_{\alpha\beta} &= 0
\end{aligned}$$

Where we have used the symmetries of the Riemann Curvature tensor, the definitions of the Ricci scalar and tensor the fact that the covariant derivative of the metric is zeros as well as relabelled the two latter terms. From this we can relabel and extract the identity:

$$D^\mu \left(R_{\mu\nu} - \frac{1}{2} g_{\mu\nu} R\right) = 0$$

We can subtract our identity from our left hand side to obtain:

$$\left(A_c + \frac{1}{2}\right) D_\mu R = 0$$

And since the ricci scalar is generally not constant, we have that $A_c = -1/2$.

To obtain our second constant we rewrite our equation:

$$R_{\mu\nu} = B_c \left(T_{\mu\nu} - \frac{1}{2} g_{\mu\nu} g^{\rho\sigma} T_{\rho\sigma}\right)$$

Here we have used that contracting our original equation with the metric and taking the trace gave us:

$$R = -B_c g^{\mu\nu} T_{\mu\nu}$$

And simply inserted that. From here we consider the Newtonian limit. Here, the metric is independent of time, the gravitational field is weak and the velocities in

question are much smaller than c. For Newtonian matter our Energy momentum tensor reduces to $T_{\mu\nu} = T_{00} = \rho$ and our equation reduces to:

$$R_{00} = \frac{1}{2} B_c \rho$$

In the Newtonian limit we furthermore can compute the Ricci scalar:

$$R_{00} = R^{\mu}_{0\mu 0} = R^{i}_{0i0} \tag{3}$$

Since the Riemann curvature symmetries implies that $R^0_{000} = 0$.

We see that in our limit the Ricci scalar reduces to:

$$R^i_{0i0} = \partial_i \Gamma^i_{00} = -\frac{1}{2} \partial_i \partial^i h_{00} = -\frac{1}{2} \overline{\nabla}^2 h_{00}$$

We can compare this to the result for the newtonian limit of the geodesics equation. Here we find:

$$R_{00} = \nabla^2 \phi$$

We can thus write:

$$\nabla^2 \phi = \frac{1}{2} B_c \rho$$

We can compare this to the poisson equation $\nabla^2 \phi = 4\pi G \rho$ and since we are in the weak field limit we realise these should be the same. We can thus see that:

$$B_c = 8\pi G$$

Putting it all together we have:

$$R_{\mu\nu} - \frac{1}{2} g_{\mu\nu} R = 8\pi G T_{\mu\nu}$$

This is the Einstein Field Equation and describe the motion of relativistic particles in the presence of gravitational fields. Note that this equation is in fact 10 coupled differential equations and is thus not easily solved for any particular matter distribution. As we shall see later it becomes necessary to make some approximations to reduce the complexity of the calculations. One of such schemes, which we shall use is the Post-Newtonian approximation which will be explained later.

2.4 Gravitational waves

In the weak field limit the Einstein Field Equations is reduced to the much simpler form:

$$\Box h_{\mu\nu} = -16\pi G \left(T_{\mu\nu} - \frac{1}{2} \eta_{\mu\nu} \eta^{\rho\sigma} T_{\rho\sigma} \right)$$

Where $\Box = \partial^\mu \partial_\mu = \frac{1}{c^2}\frac{\partial^2}{\partial t} - \nabla^2$ being the d'Alambertian operator, $T_{\mu\nu}$ is the Stress-Energy Tensor and G the gravitational constant. Considering the vacuum equation this becomes:

$$\Box h_{\mu\nu} = 0$$

For which one can make an anzats for a wave solution:

$$h_{\mu\nu}(x) = A_{\mu\nu} \exp\left(ik_\rho x^\rho\right)$$

Since we know that the metric perturbation is symmetric $h_{\mu\nu} = h_{\nu\mu}$ we must impose this on our solution as well leading to $A_{\mu\nu} = A_{\nu\mu}$. Our solution furthermore must satisfy the Lorentz Gauge condition which imposes the following:

$$k^\mu A_\mu \nu = \frac{1}{2} k_\nu \eta^{\rho\sigma} A_{\rho\sigma}$$

Inserting our solution into the vacuum equation we obtain:

$$\begin{aligned} \Box h_{\mu\nu} &= 0 \\ \partial_\alpha \partial^\alpha A_{\mu\nu} \exp(ik_\rho x^\rho) &= 0 \\ i^2 k_\alpha k^\alpha A_{\mu\nu} \exp(ik_\rho x^\rho) &= 0 \\ -k_\alpha k^\alpha h_{\mu\nu} &= 0 \end{aligned}$$

As $h_{\mu\nu}$ is generally non-zero the only way for this equation to be true is if:

$$k_\mu k^\mu = 0$$

This corresponds to a monochromatic plane wave propagating at the speed of light.

One can see that our solution has 16 components, with each unique component corresponding to a physical polarisation of the gravitation waves. However by imposing the following constraints:

$$A_{\mu\nu} = A_{\nu\mu}, \quad A_{\mu 0} = 0, \quad \eta^{\mu\nu} A_{\mu\nu} = 0, \quad k^\mu A_{\mu\nu} = 0, \quad k_\mu k^\mu = 0$$

We are reduced to only two physically distinct wave polarisation.

2.4.1 Binary GW radiation

For non-relativistic sources for GW, like Black hole Binaries, the energy emitted obeys the Einstein Quadropole formula:

$$\frac{dE_{\text{rad}}}{dt} = \frac{G}{5c^5} \left(\frac{d^3 I_{ij}}{dt^3} \right)^2$$

with I_{ij} being the mass quadropole moment given by the integral of the newtonian mass density over a compact region of space:

$$I_{ij} = \int_{\text{source}} d^3 r \left(r_i r_j - \frac{1}{3} \delta_{ij} r^2 \right) T_{00}(t, \boldsymbol{x})$$

From this it can be shown that for a binary system the average power emitted is given as[1]:

$$\frac{dE_{\text{rad}}}{dt} = \frac{32}{5}\frac{G^4\mu^2M^3}{c^5a^5}F(e)$$
$$F(e) = (1-e^2)^{-7/2}\left(1+\frac{73}{24}e^2+\frac{37}{96}e^4\right)$$

Where e is the orbital eccentricity, $\mu = GM$ and M the total binary mass. This means that over time the binary will radiate away all its rotational and gravitational energy in the form of gravitational waves.

It can furthermore be shown that the average angular momentum flux is:

$$\frac{dJ_{\text{rad}}}{dt} = \frac{32}{5}\frac{G^{7/2}\mu^2M^{5/2}}{a^{7/2}}(1-e^2)^{-2}\left(1+\frac{7}{8}e^2\right)$$

With a the semi-major axis (SMA). For a binary orbit we can write the total energy as:

$$E = -\frac{GM\mu}{2a}$$

Taking the energy flux of this system we obtain:

$$\frac{dE}{dt} = -\frac{GM\mu}{2}\frac{d}{dt}\left(\frac{1}{a}\right) = \frac{GM\mu}{2a^2}\frac{da}{dt}$$

And since we know that the only energy lost is due to gravitational radiation we have:

$$\frac{dE}{dt} = -\frac{dE_{\text{rad}}}{dt}$$
$$\frac{GM\mu}{2a^2}\frac{da}{dt} = -\frac{32}{5}\frac{G^4\mu^2M^3}{a^5}F(e)$$
$$\frac{da}{dt} = -\frac{64}{5}\frac{G^3\mu M^2}{a^3}F(e)$$

By similar procedure we can obtain the eccentricity flux since we know that:

$$J = \mu\sqrt{GMa(1-e^2)}$$
$$\frac{dJ}{dt} = \mu\sqrt{GM}\left(\sqrt{\frac{1-e^2}{2a}}\frac{da}{dt}+\sqrt{\frac{ae^2}{1-e^2}}\frac{de}{dt}\right)$$
$$= -\mu\sqrt{GM}\left(\sqrt{\frac{1-e^2}{a}}\frac{32}{5}\frac{G^3\mu M^2}{a^3}F(e)+\sqrt{e\frac{a}{1-e^2}}\frac{de}{dt}\right)$$

We again notice that the angular momentum flux must be the negative of the gravitational radiation angular momentum flux.

$$\frac{dJ_{\text{rad}}}{dt} = -\frac{dJ}{dt}$$

Which we can simplify to obtain:

$$\frac{de}{dt} = -\frac{304}{15}\frac{G^3\mu M^2}{a^4}e(1-e^2)^{5/2}\left(1+\frac{121}{304}e^2\right)$$

from the SMA flux and the eccentricity flux we see that the gravitational waves drive circularization through inspiral.

Solving the semi major axis equation we obtain:

$$a_0 = \left(\frac{256}{5}G^3\mu M^2 F(e) t_{\text{inspiral}}\right)^{1/4}$$

We can input the Hubble time to see what the initial distance must be for two black holes orbiting each other to merge in that time. We obtain that for $t_H = 14.4$ GYr two black holes with equal mass $M = 50\ \mathrm{M}_\odot$ in a perfectly circular orbit should start out at a distance of of the order 0.01 AU which is a significant problem as binary stars would not be able to form binary black holes with that distance unassisted.

By combining the two differential equations we can obtain the following equation:

$$\frac{da}{de} = \frac{12}{19}\frac{a}{e}\frac{1+\frac{73}{24}e^2+\frac{37}{96}e^4}{(1-e^2)\left(1+\frac{121}{304}e^2\right)}$$

Solving this equation we obtain:

$$\begin{aligned}
\int\frac{da}{a} &= \int\frac{de}{e}\frac{12}{19}\frac{1+\frac{73}{24}e^2+\frac{37}{96}e^4}{(1-e^2)\left(1+\frac{121}{304}e^2\right)} \\
\ln(a) &= \ln\left((e^2-1)^{-1}\right)+\ln\left(e^{12/19}\right)+\ln\left((121e^2+304)^{870/2299}\right)+\widetilde{C_0} \\
a(e) &= \frac{C_0 e^{12/19}}{(1-e^2)}\left(1+\frac{121}{304}e^2\right)^{870/2299}
\end{aligned}$$

Where C_0 is a constant of dimensions of length that is determined by the initial conditions. From this we can see that when $e \approx 1$ our dominating factor becomes $(1-e^2)^{-1}$. Because of this we expect that in the high eccentricity limit our semi major axis must change by many orders of magnitude before any significant drop in eccentricity is expected. This can be seen in figure (4):

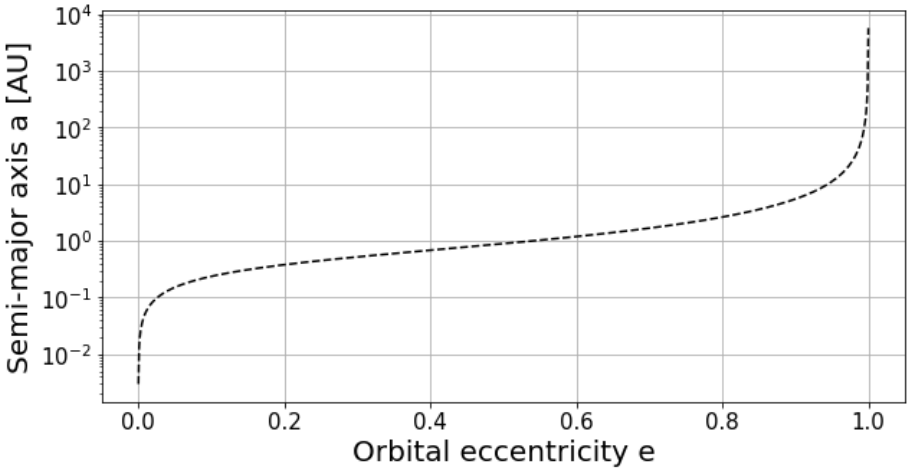

Figure 4: Graph of the analytical solution of the function $a(e)$. Notice the asymptotic behaviour around $e = 1$ which is to be expected, since in the high eccentricity limit, our function scales as $(1 - e^2)^{-1}$.

These functions will be used to check the simulations for regions of validity as we should expect these behaviours to hold for any binary. As we shall see later on, the simulation does conform to this within the region we are interested in, but diverges for sufficiently small SMA.

2.5 Post-Newtonian Expansion

As previously discussed the weak field approximation we could write the metric as a perturbation of the Minkowski-metric:

$$g_{\mu\nu} = \eta_{\mu\nu} + h_{\mu\nu}(x)$$

Which resulted in the much simpler Einstein Field equation:

$$\Box h_{\mu\nu} = -\frac{16\pi G}{c^4}\tau_{\mu\nu}$$

with $\tau_{\mu\nu} = T_{\mu\nu} - \frac{1}{2}\eta_{\mu\nu}\eta^{\rho\sigma}T_{\rho\sigma}$ being the gravitational source term. Now suppose our matter distribution $T_{\mu\nu}$ can be expanded as[5]:

$$T^{\mu\nu} = \sum_{n}^{\infty} \frac{1}{c^n} T^{\mu\nu}_{(n)}$$

with (n) being the n'th order of the matter distribution. Since these sources are slow and weak self gravitating the metric field is generated from very slow matter $v/c \ll 1$. As such the change in the metric field as a function of time is much smaller than the change in space. As such we can reduce our D'Alembertian

operator to a simple Laplacian. Expanding the metric perturbation $h_{\mu\nu}$ and the gravitational source term $\tau_{\mu\nu}$ we get:

$$h^{\mu\nu} = \sum_{n=2}^{\infty} \frac{1}{c^n} h^{\mu\nu}_{(n)}$$
$$\tau^{\mu\nu} = \sum_{n=-2}^{\infty} \frac{1}{c^n} \tau^{\mu\nu}_{(n)}$$

we can then put all of this together to obtain the recursive formula for the series expansion:

$$\nabla^2 h^{\mu\nu}_{(n)} = 16G\tau^{\mu\nu}_{(n-4)} + \partial_t^2 h^{\mu\nu}_{(n-2)}$$

And since we know that our equations of motion in general relativity is the geodesic equation which depends upon the derivatives of the metric, we now have a formalism for the acceleration of objects in terms of Post-Newtonian terms.

Expanding in the ratio between the velocity of the object and the speed of light c we can express the acceleration experienced by an object of mass m_1 by another object m_2 as the series:

$$\mathbf{a} = \mathbf{a_0} + c^{-2}\mathbf{a_2} + c^{-4}\mathbf{a_4} + \mathbf{a_5} + \mathcal{O}(c^{-6})$$

Where $a_0 = Gm_2/r_{12}^2$ is the Newtonian potential. The first Post-Newtonian (PN) term is a_2 which, along with a_4, account for periastron shift. a_5 also known as the 2.5 PN term is given as[5]:

$$\mathbf{a_5} = \frac{4}{5}\frac{G^2 m_1 m_2}{r_{12}^3}\left[\left(\frac{1Gm_1}{r_{12}} - \frac{8Gm_2}{r_{12}} - v_{12}^2\right)\mathbf{v_{12}} + (\hat{\mathbf{r}}_{\mathbf{12}} \cdot \mathbf{v_{12}})\left(\frac{52Gm_2}{3r_{12}} - \frac{6Gm_1}{r_{12}} + 3v_{12}^2\right)\hat{\mathbf{r}}_{\mathbf{12}}\right]$$

and is very important to our numerical simulations. Looking at the 2.5PN term for circular binary orbit we have $\hat{\mathbf{r}}_{\mathbf{12}} \cdot \mathbf{v_{12}} = 0$ meaning our formula reduces to only the first term. Taking $m_1 = m_2 = m$ we see that our acceleration contribution becomes:

$$\mathbf{a_5}(e = 0, m_1 = m_2 = m) = -\frac{4}{5}\frac{G^2 m^2}{r^3}\left(\frac{6Gm}{r} + v^2\right)\mathbf{v}$$

which will be a negative number, acting as a drag force given as:

$$F_{2.5\mathrm{PN}} = mc^{-5}a_5 = \frac{32\sqrt{2}}{5}\frac{G^{7/2}}{c^5}\left(\frac{m}{r}\right)^{9/2}$$

Here we have substituted in the orbital velocity $v = \sqrt{2Gm/r}$.

In our numerical simulation we will refrain from using the contributions from lower order corrections, instead relying on the acceleration:

$$\mathbf{a} = \mathbf{a_0} + c^{-5}\mathbf{a_5}$$

The modified acceleration is however only strictly valid for number of objects $N \leqslant 2$. However this approach can still be used for $N > 2$ objects without introducing significant error, since our 2.5PN contribution has a much steeper dependence on the separation than the Newtonian part ($a_5 \propto r^{-9/2}$ vs $a_0 \propto r^{-2}$). Thus the closest pair contribution will always dominate.

Since our 2.5PN term is the first Post-Newtonian term that acts like an energy-sink, ie takes energy away from the system in the form of shrinkage of the SMA as well as loss of angular momentum resulting in circularisation of the orbit. As such one should find a general agreement between a simulated binary and the theoretical behaviour from the Quadropole formalism.

3 Stellar Evolution

This section will cover the different sources for BBH mergers as well as describe the environment of the Active Galactic Nuclear (AGN) disk which, in a simplified form, will be the subject of the numerical results obtained later on.

We begin by covering the different evolution channels for BBH formation. As the topic of this thesis is one particular case of BBH formation this section will not dwell too much on each channel. Note also that this will not be an exhaustive list as this is still an active area of research.

3.1 Separate Evolution

The simplest evolution channel is the separate evolution channel. Consider a Stellar Binary with semi major axis at such a scale that while the two stars are bound, their evolution from star to black hole can be considered as an isolated event. These binary black hole formations, while valid, will not produce any gravitational waves on their own. As we have previously discussed, the energy loss rate due to gravitational waves is proportional to a^{-5} meaning that at distances $a \gg 1$ AU the radiation rate is suppressed to the point that nothing will be detectable in the LIGO VIRGO band.

3.2 Common Evolution

For common evolutions the BBH is directly formed from an existing Stellar Binary and through different mechanisms are kept together while going through the stellar evolution, thus being able to undergo a BBH merger in a Hubble time.

3.2.1 Common Envelope Channel

In the common evolution (CE) channel the distance between the binary stars is much smaller than the separate evolution channel. As the two stars goes through their evolution they will inevitably interact with each other.

The binary potential on a test mass m at a distance r from a stable binary we have:

$$U_{\text{Binary}} = -\frac{m\mu}{r} - \frac{1}{2}m\omega^2 r^2$$

We can, of course equate this with $U = m\Phi$ where Φ is the effective gravitational potential. We can thus find a point between the binaries for which.

$$\mathbf{F} = -m\nabla\Phi = 0$$

known as the Lagrange point L_1. This point will be important as it will be through this that mass can flow from one star to the other. Define the Roche Lobes as a figure eight shaped surface with each star at the center of each lobe and the crossing point being at L_1. Suppose material passe through the Roche Lobes at any other point than L_1. By the shape of the surface it must now be located in a lobe with one of the stars at its center. The usefulness of the Roche Lobes is that once through the surface, the material will have a stronger gravitational attraction to the star in the lobe than the other, meaning the mass would inevitably pass to the star at the center of said lobe. The exact shape of the lobes will not be examined further in this thesis as it it does not have an analytical solution.

The question now becomes: What happens if one of the stars exceeds its Roche Lobe? This will happen at some point as, once the star in question has exhausted its fuel, it will expand becoming a red super giant. As the Roche Lobe is filled mass will be ejected from the giant, some of which will flow to the smaller star through L_1. For a giant star filling its Roche Lobe with mass M_G and a smaller star with mass $M_\star$ it can be shown that through this mechanism the orbit evolves as:

$$\frac{\dot{a}}{a} = -2\left(1 + [\beta - 1]\frac{M_G}{M_\star}\right)\frac{\dot{M}_G}{M_G}$$

Where β is the fraction of ejected matter which leaves the system. We can see from this that for $\beta = 0$, that is when all matter ejected from M_G is captured by $M_\star$ the semi major axis will evolve as:

$$\frac{\dot{a}}{a} = \begin{cases} > 0 & \text{for } M_G < M_\star \\ = 0 & \text{for } M_G = M_\star \\ < 0 & \text{for } M_G > M_\star \end{cases}$$

Moving further along in the evolution of the Giant star, it will at some point undergo a Super Nova (SN) explosion. During this process, it will not only eject

the majority of its stellar material, leaving behind either a Neutron Star or a Black hole. The SN explosion is instantaneous compared to the orbital period of the binary system and in general asymmetric and anisotropic. As such, the explosion will impart a kick on the remnant in the form of a recoil velocity $\mathbf{v}_{\text{kick}}$. Depending on how one models the distribution of these SN kicks, a portion of the stellar binaries will be destroyed. This is, however, still an active area of research and not one that will be the focus of this thesis. Should the binary survive, the second star will undergo the same evolution becoming a giant. At this point the mass transfer will shift as the stellar remnant now becomes the receiver of the mass transfer from the new giant. Inevitably the mass transfer from the giant to the stellar remnant becomes unstable as the remnant cannot absorb the matter quickly enough leading to the giant absorbing the stellar remnant in a common envelope. The CE extracts energy from the binary orbit via dynamical friction eventually unbinding itself from the system. By considering the energy before and after the unbinding of the envelope one can show the change in scale of the orbital radius to be:

$$\frac{a_f}{a_i} = \frac{M_{\text{Core}}}{M_{\text{G}}} \left(1 + \frac{2}{\lambda\alpha} \frac{a_i}{R_L} \frac{M_{\text{env}}}{M_{\text{SR}}}\right)$$

Where M_{Core} and $M_{\text{env}}$is the mass of the core and envelope of the stellar giant, M_{SR} is the mass of the stellar remnant, and λ and α are dimensionless parameters pertaining to the density profile of the envelope and the efficiency of orbital energy expenditure. Back of the envelope calculations can show that:

$$\frac{a_f}{a_i} \sim 10^{-3} - 10^{-2}$$

At this stage in the common evolution the orbital distance will be so small that when the second SN kick occurs, most binaries will survive. At this point the stellar remnant binary will be close enough to merge within a Hubble time[7].

3.2.2 Chemically-Homogenous Evolution Channel

In the Chemically-Homogenous Evolution we instead imagine our two stars in a binary rotating rapidly around their own axis. This rotation cannot be in hydrostatic and radiative thermal equilibrium leading to a mixing of the internal layers of the stars. This can lead to a whole other evolution path than would be expected. Stars that rotate slowly would tend to form a composition gradient insides, with a Helium rich core and a Hydrogen rich envelope. As the core contracts during the evolution, hydrostatic and thermal equilibrium is maintained by the envelope expanding which, if in a binary, could lead to an overfilled Roche-Lobe and resulting mass transfer as per previous section. The rapidly rotating star would instead mix the core and envelope meaning no gradient would form and the star would instead maintain an almost constant radius throughout its main sequence evolution. As the Hydrogen is burned up throughout the star, it will start to contract as it moved to a Helium burning

star of lower radius. The star will then continually contract as the Helium is expended eventually contracting to become a stellar mass black hole. This has been shown to be possible for equal mass stellar binaries if they are sufficiently massive (object mass $M \gtrsim 30\ M_\odot$) and sufficiently high individual rotational frequency ($T \lesssim 1$ Day)[6][4].

3.3 Dynamical Evolution

While Common evolution dealt with a single binary operating in a vacuum, dynamical evolution takes the environment into account. This section includes different evolution channels, but for our purpose we are interested in the Binary-Single interactions or, the 3-body system as we will refer to it as for the remainder of this project.

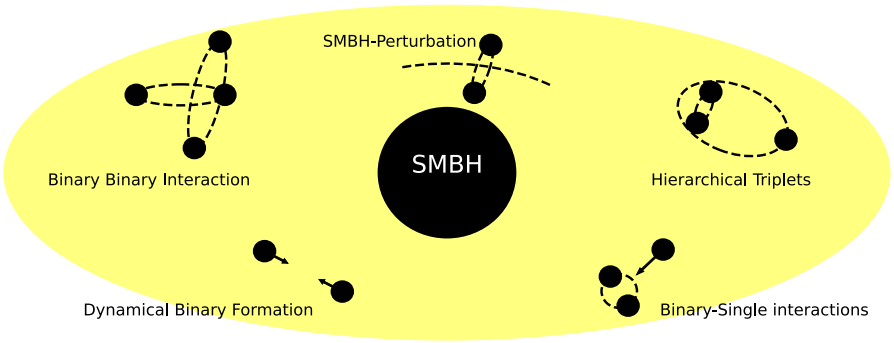

Figure 5: AGN disk with different merger channels drawn.

Briefly, some of the other channels proposed are:

- **Binary Binary Interactions**
  Two BBHs, one orbiting the other, interact with each-other resulting in modified SMAs leading to inspiral within a Hubble-time[10]
- **SMBH-Perturbation**
  In the presence of the SMBH the eccentricity and SMA of an otherwise stable binary can be perturbed leading to inspiral within a Hubble-time
- **Dynamical Binary Formation**
  Two BHs experience a close interaction leading to either a collision and merger or a new binary with SMA and eccentricity, enabling the inspiral within a Hubble-time[11]
- **Hierarchical Triplets**
  A binary with a singlet orbiting the binary, enabling perturbation of the SMA and eccentricity of the BBH leading to inspiral within a Hubble-time[9]

These channels are beyond the scope of this project and we will move on to the 3-body interactions.

3.4 3-Body interactions

3 Body stellar encounters can be divided into three main categories describing the interactions of compact objects in space which includes BHs.

- **Weak Perturbation (WP)** in which the singlet passes the binary at a hyperbolic trajectory at a large distance compared to the binary semi major axis. The passage time for this encounter is larger than the orbital period of the binary leading to a weak perturbation of the binary. This is the most common encounter.
- **Strong Perturbation (SP)** in which the singlet passes the binary at a hyperbolic trajectory at a distance comparable to the semi-major axis of the binary. The passage time here is less than or equal to the orbital period and should have a greater effect on the binary.
- **Close Encounter (CI)** in which the singlet will pass the binary at at distance to the binary center comparable to the binary separation. In this case all three objects will have similar gravitational strength compared to one another and the outcome will be chaotic.

In this project we will refrain from looking at the perturbative interactions and focus solely on CI.

We define CI's as occurring when a third body passes the binary center of mass at a distance $r_{\rm CI} = 2\frac{m_H}{M}a$ with m_H being the heavier binary element and M being the total binary mass. From here we see that for our equal mass case ($m_H = m$, $M = 2m$) this reduces to $r_{\rm CI} = a$ that is, our third object passing within a distance comparable to the binary separation itself.

The setup for the third body initial conditions will be expounded upon in a later section but for now, suffice to say that by treating the binary as as single object with mass M located at the center of mass of the binary itself the closest approach of the third body corresponds to an impact parameter b which can be found by energy and angular momentum conservation to be:

$$b(r_{\rm min}) = r_{\rm min}\sqrt{1 + \frac{6Gm}{r_{\rm min}v_\infty^2}} \tag{4}$$

where v_∞ is the speed of the third object when approaching from infinity and $r_{\rm min}$ is the smallest distance between the singlet and the binary center of mass. We see that any encounter with $b = b(r_{\rm CI})$ will correspond to $r_{\rm min} < r_{\rm CI}$. From this we can conclude that all CI's must happen for $r_{\rm min} \leqslant r_{\rm CI}$ meaning all encounters coming from within the area $\sigma_{\rm CI} = \pi b(r_{\rm CI})^2$ must lead to a CI. This area is defined as the cross-section for CI's. Expanding it we obtain:

$$\sigma_{\rm CI} = \pi r_{\rm CI}^2\left(1 + \frac{6Gm}{r_{\rm CI}v_\infty^2}\right) \tag{5}$$

Depending on the relative binding energy of the binary and the kinetic energy of the third object, we will see that either the first (Geometric) term of second (Gravitational) term will dominate. From the binary we can extrapolate an approximate interaction rate. Assuming an isotropic stellar density n with the average relative velocity $\langle v \rangle = v_\infty$ we have the rate:

$$\Gamma \simeq n\sigma_{\mathrm{CI}} v_\infty \tag{6}$$

Which is the theoretical rate of CIs. We see here that our CI rate depends solely on the cross section. Much work has been done by Samsing and D'Orazio in [3] to determine the cross section of the outcomes of 3 body interactions the main results of which we are interested in is the merger cross section given as:

$$\sigma_{\mathrm{merger}} = P_{\mathrm{merger}} \sigma_{\mathrm{CI}} \tag{7}$$

The merger probability is thus the only truly unknown and the one this thesis strives to determine.

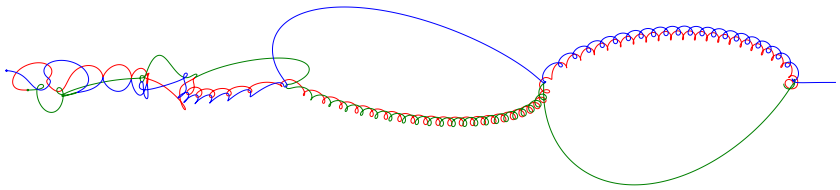

Figure 6: an example of a 3-body merger.

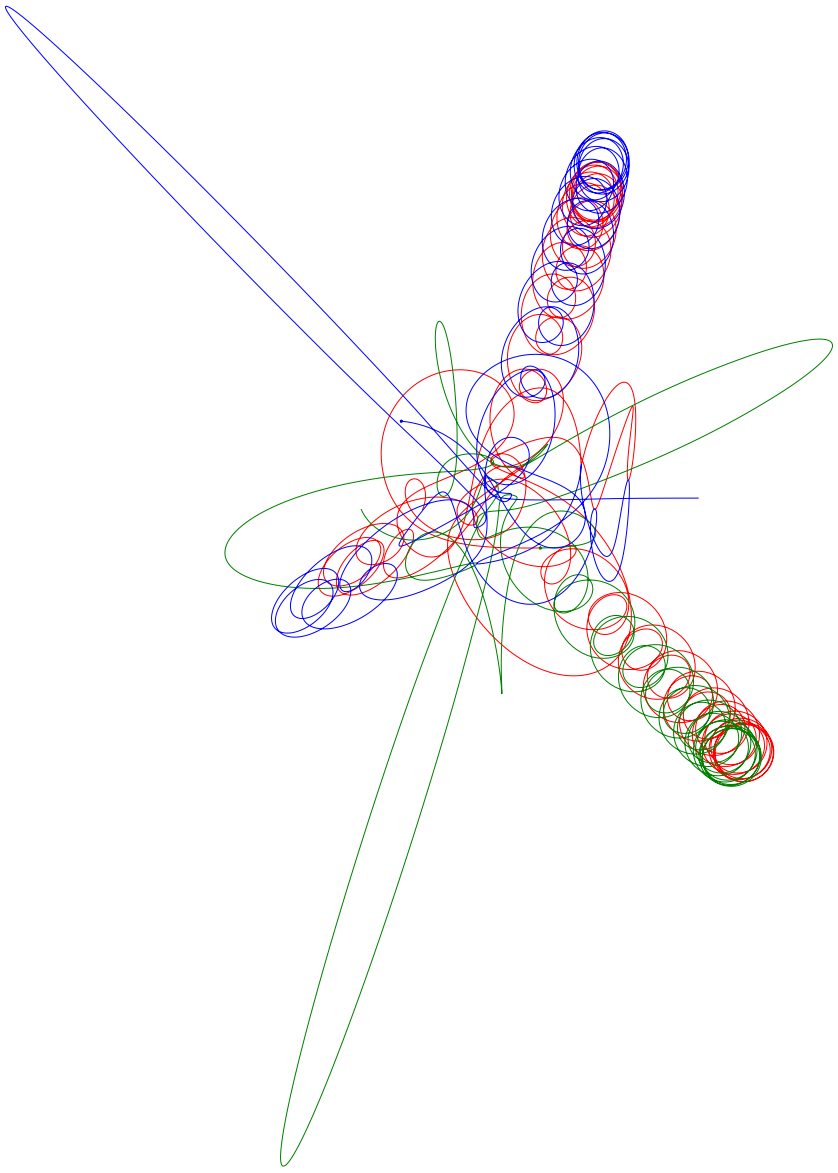

Figure 7: 3-body merger seen in the COM frame of the 3-body system

3.5 Derivation of merger probabilities

This thesis only seek to investigate the merger rates for 2D disk interactions. As such the general 3 body interactions becomes a lot simpler. We have two different channels for mergers:

- **The 2 Body merger** in which, after interacting chaotically, a BH is ejected from the system, and a binary is formed which will inspiral.

- **The 3 Body merger** in which two BH inspiral while still gravitationally bound to a BH singlet

We begin by considering the timescale for which an eccentric BBH will merge. This is shown to be[1]:

$$t_{\text{inspiral}} = \frac{5c^5}{256G^3}\frac{a^4}{\mu M^2 F(e)} \approx \underbrace{\frac{5c^5}{512G^3}\frac{a^4}{m^3}}_{t_c}(1-e^2)^{7/2} \tag{8}$$

Where a, e and m are initial semi major axis, eccentricity and black hole mass of the system. In the last equality we have used the equal mass case $m_1 = m_2 = m$ and the high eccentricity approximation $F(e) \approx (1-e^2)^{-7/2}$.

For planar restricted 3 body interactions one can show that the distribution of eccentricities are given as[2]:

$$P(e) = \frac{e}{\sqrt{1-e^2}} \tag{9}$$

Suppose we wanted to know the probability of our eccentricity being larger than some choice eccentricity e_0. For this we have:

$$p(e > e_0) = \int_{e_0}^{1} P(e)de = \sqrt{1-e_0^2} \tag{10}$$

Since we know the relationship between t_{inspiral} and the eccentricity we can simply associate $\sqrt{1-e_0^2}$ with some timescale τ to obtain:

$$p(t_{\text{inspiral}} < \tau) = \left(\frac{\tau}{t_c}\right)^{1/7} = \left(\frac{512G^3\tau}{5c^5}\right)^{1/7} a^{-4/7}m^{3/7} \tag{11}$$

This is our probability function for merger of two binary black holes within a set timescale τ as a function of the initial semi major axis a and mass of each black hole m.

Substituting in the average interaction time $\tau = t_i = 10^5$ Yr and expressing this in terms of normalised parameters which will be used in this thesis:

$$p_2 \approx 0.09\left(\frac{t_i}{10^5\ \text{yr}}\right)^{1/7}\left(\frac{m}{50M_\odot}\right)^{3/7}\left(\frac{a}{1\ \text{AU}}\right)^{-4/7} \tag{12}$$

For the 3 body merger it has been shown that one can express the chaotic interactions as a series of temporary binary-single states. In order for a merger to take place it must happen in one of these temporary states, which has the characteristic timescale of the orbital period of the initial binary $T = 2\pi\sqrt{a_0^3/Gm}$. From here we can simply utilise the same logic as before to obtain:

$$p_3 = N\left(\frac{T}{t_c}\right)^{1/7} = N\left(\frac{1024\pi G^{5/2}}{5c^5}\right)^{1/7} a^{-5/14} m^{5/14} \tag{13}$$

Where N is the average number of interactions that will be determined numerically. In normalised units this becomes:

$$p_3 = N \cdot 0.014\left(\frac{m}{50\mathrm{M}_\odot}\right)^{5/14}\left(\frac{a}{1\ \mathrm{AU}}\right)^{-5/14} \tag{14}$$

We thus have the probabilities of the 2- and 3-body mergers proportional to the initial separation of circular orbit binaries to some power. From this we see that for small enough a our results should be dominated by the 2 body mergers while for larger initial distance the 3 body mergers will make up the vast majority. The initial distance a_c for this change should be at $p_2/p_3 = 1$ for which we have:

$$a_c = \frac{N^{-14/3}}{(2\pi)^{2/3}} G^{1/3} m^{1/3} t_i^{2/3} = 2153 N^{-14/3}\ \mathrm{AU}\left(\frac{m}{50M_\odot}\right)^{1/3}\left(\frac{t_i}{10^5\ \mathrm{yr}}\right)^{2/3} \tag{15}$$

We see here that this critical point is extremely dependent upon the numerical value of N due to the $-14/3$ power. As such the critical point will end up with an uncertainty spanning multiple orders of magnitude. A value for this has been found by Samsing to be $N = 20$[8] but for now we shall leave this as uncertain and dependent upon the simulation in question. As such we will obtain our own later on.

Plotting the probability distributions we get the following figure:

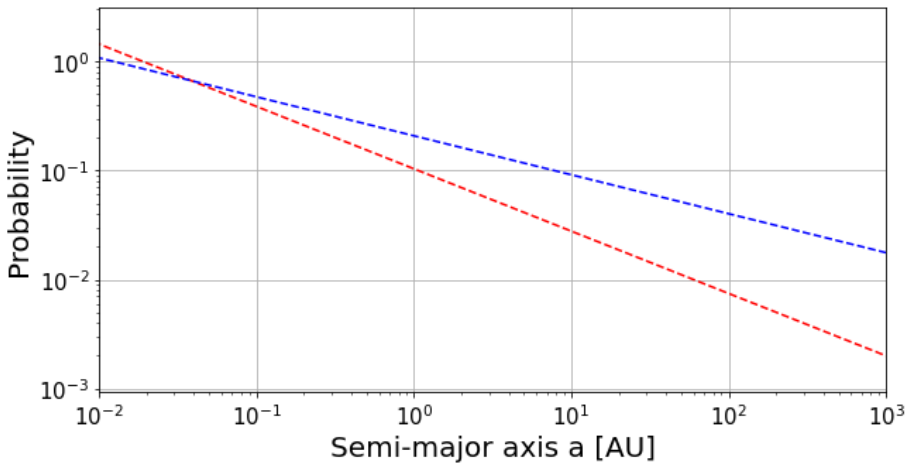

Figure 8: The probability distributions of the 2 body merger p_2 and 3 body merger p_3 on a log log diagram.

We shall use this to verify the functionality of our 3-body simulations in a vacuum later on. They will furthermore be held up against the results presented by Samsing et al [8] for similar reasons.

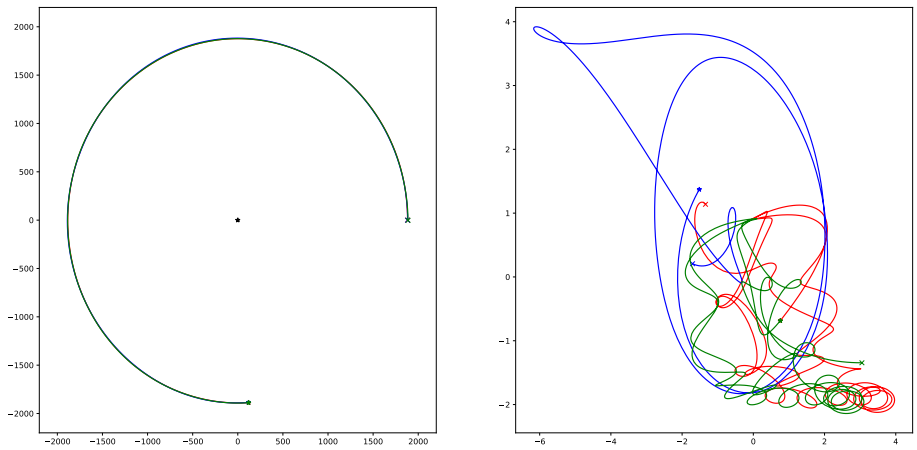

Figure 9: 3-body merger in an SMBH environment. This is at a distance of 2 tidal radii with the SMA being 1 AU.

3.6 Super Massive Black Holes

At the center of AGNs we find the gravitational anchor: The Super-Massive Black Hole. This section will describe the relevant parameters used to implement the SMBH in our simulation. As can be seen below, the introduction of the SMBH, changes the trajectory of the 3-body system greatly. Compared to fig. (**??**) and (7). Below we see a 3-body merger but the COM motion is significantly altered compared to the vacuum case:

3.6.1 Newtonian potential

We define ΔR as the initial distance between the BBH center of mass and the position of the SMBH. For $R \gg \Delta a_0$ can assume to work in a near Newtonian environment and as such can simplify to a Newtonian potential with the acceleration on the i'th body being.

$$\mathbf{a}_{\mathrm{SMBH,i}} = -\frac{\mu}{r_i^2}\hat{\mathbf{r}}_\mathbf{i} \tag{16}$$

with $\mu = GM_{\mathrm{SMBH}}$. Since our implementation requires our 3 body system to be in a stable orbit we also define the center of mass velocity to be:

$$v_{\mathrm{COM,SMBH}} = \sqrt{\frac{GM_{\mathrm{SMBH}}}{R}} \tag{17}$$

Where R is the distance from the center of mass to the SMBH. This distance is of interest to us as it will be the variable parameter when testing the SMBH impact upon the 3 body merger probabilities. The distance will be done as a multiple of the tidal disruption radius which we will now explore.

3.6.2 Tidal Disruption and regions of gravitational dominance

In order to make sure we do not tear apart the 3 body system we must operate at some scalar of the systems tidal disruption radius. Tidal disruption is the phenomenon where a celestial body (e.g. a star) moves sufficiently close to a SMBH to be pulled apart along the line towards the SMBH. For a body with radius r_3 and mass $m_3 = 3 \cdot m_{\text{BH}}$ orbiting a SMBH with mass M, the tidal disruption radius is approximately given as:

$$R_{\text{Tidal Disruption}} \approx r_3 \left(\frac{M}{m_3} \right)^{1/3} \tag{18}$$

in our case the mass of our body is the mass of the 3 body system and the radius is set to be the distance from the COM to the singlet.

The Tidal disruption radius is, however, mainly useful for compact objects. For our 3 body system we must bear in mind that as the system evolves the object radius will vary. As such we need to understand the radius of gravitational dominance of our 3-body system. For this we can use the Hill Sphere. Seeing the 3-body system as an object with mass $m_3 = 3 \cdot m_{\text{BH}}$ located at the center of mass of the system we can calculate the systems Hill Sphere. This is given as:

$$r_{\text{H}} \approx R_{\text{SMBH}} \sqrt[3]{\frac{m_3}{3M_{\text{SMBH}}}} \tag{19}$$

Where $R_{\text{SMBH}} = n \cdot R_{\text{Tidal Disruption}}$ is the distance between our center of mass and the SMBH given as the tidal disruption radius from before. From here it is easy to give a formula for our radius of gravitational dominance as a function of multiples of the Tidal disruption radius:

$$r_{\text{H}} = n r_3 \sqrt[3]{\frac{1}{3}} \tag{20}$$

with r_3 being the initial radius of the 3 body system set to 5 AU and n the scalar of the distance.

3.6.3 SMBH probability derivation

It is obvious from the consideration of the Hill Radius that The evolution of the 3 body system can be divided into three ranges based on the distance to the SMBH: For sufficiently small n we will have $r_{\text{H}} < a$ meaning the entire system is unstable as not even the initial binary will remain stable. We will not look at this scale as it is expected that the merger probability should be close to 0. For $a < r_{\text{H}} < 5$ AU we have a semi stable setup where the binary is stable but the singlet can be unbound from the beginning. For 5 AU $< r_{\text{H}} < \infty$ we have the "free" case in which our distribution should approach the vacuum solution as the distance approaches infinity. These "unstable", "near", and "far" regions provide a good framework for looking at the probability functions.

The Near region

The probability function of the Near Region should be dictated by the probability of the singlet to be shielded from the SMBH in its orientation as well as the probability that any one object leaves the hill sphere orientated close to the SMBH. We can see that the probability of our singlet being shielded from the SMBH potential must be proportional to the area in the shadow of the 3 body hill sphere and it would make sense that this probability should go to 1 as $r_h \to r_3$. As such we know that this probability is the shadow area divided by the r_3 spheres area. Furthermore the probability that the singlet starts in an orientation that is stable is proportional to the circumference of the 5 AU circle we can draw from the center of the binary that is in the shadow of the hill sphere. working on this intuition we can write:

$$P_{\text{Circumference}} = \frac{\alpha r_3}{2\pi r_3} = \frac{\alpha}{2\pi} \tag{21}$$

$$P_{\text{Area}} = \frac{A_{\text{Shadow}}}{\pi r_3^2} \tag{22}$$

To find the area we need to specify what we mean by shadow. Drawing two lines from the SMBH, which are tangent to the hill sphere we define the shadow as the area of the hill sphere as well as all area between the two tangent lines and the hill sphere. This is drawn on the figure below.

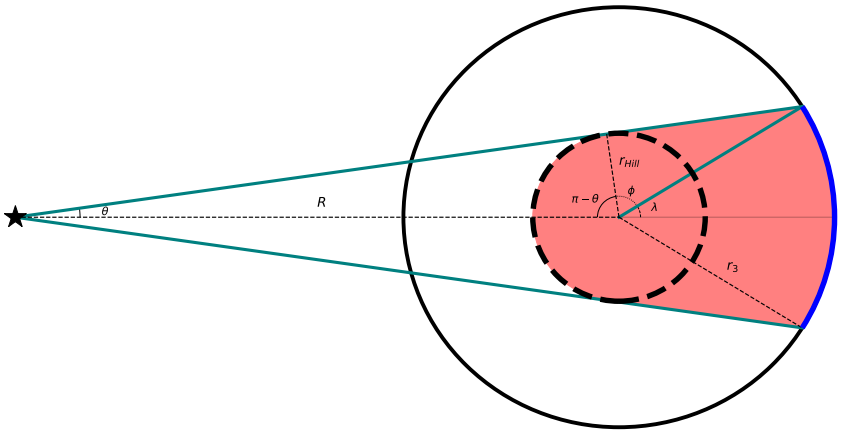

Figure 10: Schematic for the geometrical probability factors used to modify the SMBH probability function for the semi stable region.

This area can be divided into 2 sets of three parts: A section of the hill sphere, a triangle and a section of the r_3 sphere.

We can draw a triangle from the SMBH to the center of the hill sphere to the point between the hill sphere and the tangent line. From this we can calculate the angle of our hill section. We know that the angle of the tangent line and

the distance from the SMBH to the hill sphere must be:

$$\theta = \arcsin \frac{r_h}{R_{\text{SMBH}}} = \arcsin \left(\frac{m_3}{3M_{\text{SMBH}}} \right)^{1/3} \tag{23}$$

meaning our hill sphere angle must be $\pi/2 - \theta$. We can thus write our section area as:

$$A_1 = \frac{\pi/2 - \theta}{2\pi} \pi r_h^2 = \arccos \left[\left(\frac{m}{M_{\text{SMBH}}} \right)^{1/3} \right] \frac{(nr_3)^2}{2 \cdot 3^{2/3}} \tag{24}$$

Our second area consist of the tangent point to the far intersection of the tangent line and the r_3 sphere to the center of the hill sphere. For this we have the hypotenuse which is r_3 and one leg which is r_h. The angle between these two can be found as:

$$\phi = \arccos \frac{r_h}{R} = \arccos n \frac{r_3}{R} \left(\frac{1}{3} \right)^{1/3} \approx 9.42 \cdot n^2 \tag{25}$$

From this we can use the right angle area formula to obtain:

$$A_2 = \frac{1}{2} r_h R \sin \phi = \left(1 - \frac{n^2}{3^{2/3}} \right)^{1/2} \frac{n r_3^2}{2 \cdot 3^{1/3}} \approx 2.89 \sqrt{9 - 4.33 n^2} n \tag{26}$$

The area of the r_3 sphere section is now relatively easy to calculate since we know the angle must be the remainder of half a sphere subtracting the other two angles:

$$\lambda = \frac{\pi}{2} + \theta - \phi = \frac{\pi}{2} + \arcsin \left(\frac{m_3}{3M_{\text{SMBH}}} \right)^{1/3} - \arccos n \frac{r_3}{R} \left(\frac{1}{3} \right)^{1/3} \tag{27}$$

And as before the area is given as:

$$A_3 = \frac{\lambda}{2\pi} \pi R^2 = \left(\arcsin \left[\left(\frac{m}{M} \right)^{1/3} \right] + \arcsin \left[\frac{n}{3^{1/3}} \right] \right) \frac{r_3^2}{2} \tag{28}$$

$$\approx 19.69 - 12.5 \arccos(0.69n) \tag{29}$$

Along this we also need to calculate the arc length but that is easy as we just found the angle λ which spans the required arc length. We have:

$$L = 2\lambda R = 2 \left(\arcsin \left[\left(\frac{m}{M} \right)^{1/3} \right] + \arcsin \left[\frac{n}{3^{1/3}} \right] \right) r_3 \tag{30}$$

Taking the sum of the areas gives us half the red area. Multiplying by 2 and dividing by the area of the r_3 sphere will then give us the probability that our objects are in a safe configuration. The same goes for our circumference as it simply needs to be divided by the circumference of the r_3 sphere. For simplicity we can expand the probability function around $r_h = a$ which for our case means

a tidal radius factor $n = 3^{1/3}$. The expanded functions will be a lot easier to deal with numerically as well as be accurate within the region of interest, as probability function is expected to transition to the Far Region when $r_h \to r_3$. Our probability functions thus reads:

$$P_{\mathrm{A}}(n) \approx 0.0736n\sqrt{9. - 4.3266n^2} + 0.2398n^2 + 0.0012 + 0.3183 \arcsin(0.6934n) \tag{31}$$

$$\approx 0.0012 + 0.4412n + 0.2411n^2 - 0.0376n^3 + \mathcal{O}(n^4) \tag{32}$$

$$P_{\mathrm{C}}(n) \approx 0.0012 + 0.3183 \cdot \arcsin(0.6934n) \tag{33}$$

$$\approx 0.0012 + 0.2212n + 0.0020n^2 + 0.0212n^3 + \mathcal{O}(n^4) \tag{34}$$

$P_A(n)$ is the probability that during one semi ejection the singlet stays within the region of gravitational dominance of the binary. $P_C(n)$ is the probability that we start our simulation in an orientation that wont dislodge the singlet instantly. It should be noted that $P_C(n)$ only goes to $\approx 50\%$ as $r_h \to r_3$. This is simply due to the limitations of the geometric interpretation and will not become a big problem.

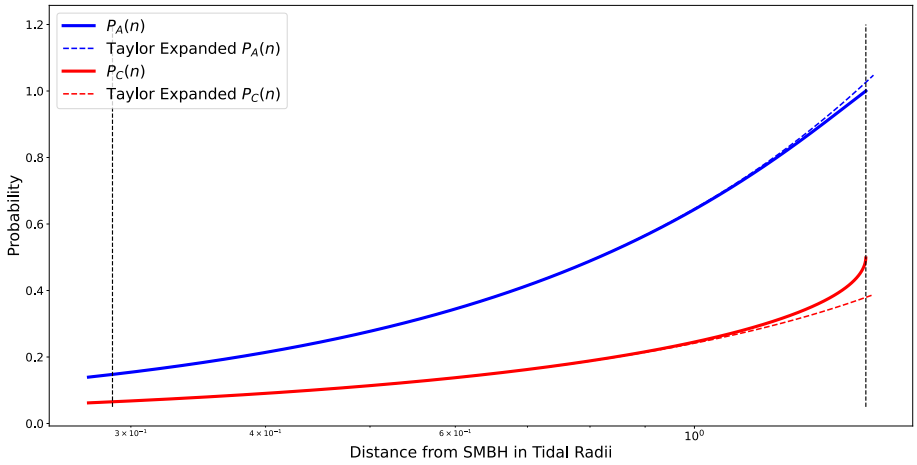

Figure 11: The Near Region probabilities to stay within the shielded area (Blue) as well as being initially oriented away from the SMBH (Red). Plotted here are also their Taylor-expansions (Dashed).

The Far Region

For the far region we can make use of the 3-body energy distribution given by [2]. For planar restricted 3-body interactions one can show that the distribution of binary absolute energies are given as:

$$P(|E_B|) = 2\frac{|E_0|^2}{|E_B|^3} \tag{35}$$

From which we can derive the probability that the binary energy is larger than some choice energy $|E_c|$:

$$p(|E_B| > |E_c|) = 2|E_0|^2 \int_{|E_c|}^{\infty} P(|E_B|) d|E_B| = \left(\frac{|E_0|}{|E_c|}\right)^2 \tag{36}$$

All that is left now is to determine this critical energy. Starting out with the simple 3 body energy and isolating for the binary energy we have:

$$|E_B| = |E_0 - E_S| \tag{37}$$

Suppose our system has undergone chaotic motion and settles into a temporary state, with a binary and a singlet currently ejected with less energy than required to escape the gravity well of the binary. This is our critical energy as it is at this point that the addition of the SMBH could dislodge the singlet and end the 3 body evolution. We know that the singlet is gravitationally bound to the binary, with $E_S < 0$. We can write up the energy of the singlet as:

$$E_S = \frac{1}{2} m v_s^2 - G\frac{2m^2}{r_s} \tag{38}$$

Since we want the singlet to be bound we know the velocity of our object must be less than the escape velocity:

$$v_s \leqslant \sqrt{G\frac{4m^2}{r_s}} \tag{39}$$

We also know that the absolute potential energy must be greater than the SMBH potential:

$$G\frac{2m^2}{r_s} \geqslant G\frac{mM}{R - r_s} \tag{40}$$

We can input both to obtain:

$$E_S \leqslant G\frac{2m^2}{r_s} - G\frac{mM}{R - r_s} = Gm\left(\frac{2m}{r_s} - \frac{M}{R - r_s}\right) \tag{41}$$

From here we chose to express the distance r_s as some scalar multiple of the SMBH distance $r_s = k \cdot R$ which will be left as a free parameter for the time being. Our energy equation becomes:

$$E_S = \frac{Gm}{R}\left(\frac{2m}{k} - \frac{M}{1-k}\right) \tag{42}$$

$$= \frac{Gm}{R}\left(\frac{2m(1-k)}{k-k^2} - \frac{Mk}{k-k^2}\right) \tag{43}$$

$$= \frac{Gm}{R}\left(\frac{2m - k(2m+M)}{k-k^2}\right) \tag{44}$$

We can also impose that $M \gg 2m$. The probability that the 3-body system survives one semi ejection thus becomes:

$$P = \frac{1}{\left(1 + \frac{Gm}{R}\left|\frac{(2m-kM)}{(k-k^2)E_0}\right|\right)^2} \tag{45}$$

3.7 Numerical considerations

3.7.1 Initial conditions

For the 3 body system we can set up the binary in a stable circular orbit around the origin with the path having some diameter a. We can set up the initial condition of the third body by examining energy- and angular momentum conservation at three different points:

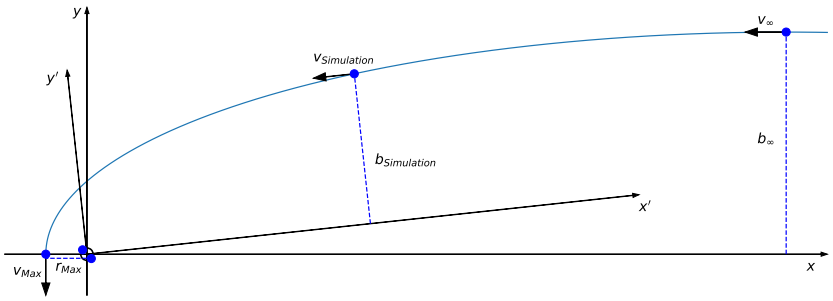

Figure 12: Illustration of the theoretical setup for our intial conditions. The binary is placed at the origin, while the relevant parameters of the singlet are obtained at three different positions: At infinite distance, at the closest distance with the binary, and the chosen distance for our simulations. The parameters of the latter is uniquely determined by the parameters of those at infinity and of the closest distance.

The first point is at infinite distance r_∞, where the gravitational energy of the binary can be neglected. Here we assume a linear path for the third body parallel to the x-axis at some offset b_∞. The assumption here is that if the binary is kept stable, the third body will trace out a hyperbolic path with focus at the origin, passing the x axis at some distance. At infinity we can write up the equation of energy and angular momentum as:

$$E_\infty = \frac{1}{2} m v_\infty^2 \tag{46}$$

$$L_\infty = m(\mathbf{r}_\infty \times \mathbf{v}_\infty) = m b_\infty v_\infty \tag{47}$$

Here we have used that the velocity is parallel to the x-axis to simplify the angular momentum.

The intersection with the x-axis is our second point of interest. At this point the third body will have the greatest velocity $\mathbf{v}_{\max}$ and be at a distance to the origin $r_{\max}$. As before we write the energy and angular momentum equations

to obtain:

$$E_{\max} = \frac{1}{2}mv_{\max}^2 - G\frac{mM}{r_{\max}} \tag{48}$$

$$L_{\max} = m(\mathbf{r}_{\max} \times \mathbf{v}_{\max}) = mr_{\max}v_{\max} \tag{49}$$

We have again used that the velocity vector and position vector here are perpendicular to each other, simplifying the cross product.

The third point of interest is that from which the simulation will be initiated. This point is chosen somewhat arbitrarily, and will be fixed later. For now we denote the distance from the origin $r_{\text{simulation}}$ and the velocity $\mathbf{v}_{\text{simulation}}$. As before we write the energy and angular momentum equation:

$$E_{\text{simulation}} = \frac{1}{2}mv_{\text{simulation}}^2 - G\frac{mM}{r_{\text{simulation}}} \tag{50}$$

$$L_{\text{simulation}} = m(\mathbf{r}_{\text{simulation}} \times \mathbf{v}_{\text{simulation}}) = mb_{\text{simulation}}v_{\text{simulation}} \tag{51}$$

Here we have simplified the angular momentum by rotating the coordinate system around the origin, such that our velocity vector is parallel to the new x-axis x'.

All that is left is to use these to find the coordinates of the third body at the start of our simulation. We set the distance to the origin to be some scalar of the semi-major axis of the binary $r_{\text{simulation}} = K \cdot a$ and the vector to be $\mathbf{r}_{\text{simulation}} = x \cdot \hat{\mathbf{i}}' + b_{\text{simulation}} \cdot \hat{\mathbf{j}}'$. By conservation of energy and angular momentum we can express our y′-component as:

$$b_{\text{simulation}} = \frac{b_\infty}{\sqrt{1 + \frac{2GM}{v_\infty^2 r_{\text{simulation}}}}} \tag{52}$$

Where $b_\infty = r_{\max}\sqrt{1 + \frac{2Gm}{v_\infty^2 r_{\max}}}$. We can now find the x′-component of our initial distance:

$$x = \sqrt{(K \cdot a)^2 - (b_{\text{simulation}})^2} \tag{53}$$

all that is left from here is to fix the velocity $\mathbf{v}_{\text{simulation}}$. In our rotated coordinate system, this vector is parallel to the x' axis and as such we can write: $\mathbf{v}_{\text{simulation}} = -v_{\text{simulation}}\hat{\mathbf{i}}'$. We can fix the speed by using conservation of angular momentum to find:

$$v_{\text{simulation}} = v_\infty \frac{b_\infty}{b_{\text{simulation}}} = v_\infty\sqrt{1 + \frac{2GM}{v_\infty^2 r_{\text{simulation}}}} \tag{54}$$

As can be seen, this is not dependant upon the impact parameter at infinity b_∞. We intend to randomly vary b_∞ in the interval $\{-b_\infty, b_\infty\}$ and if our initial velocity was sufficiently high there would be a lot of missed CI's as the impact parameter approached 0. This is, however, not a major concern here as we have chosen our velocity such that $v_\infty \ll v_{\text{binary}}$.

3.7.2 Termination conditions

In order to end the simulation it is necessary to determine weather the BHs will merge or not. In order to see if any two objects have merged, we define a new SMA a_{merge}, such that $a_{\text{merge}} = a_0/k < a_0$ with k being chosen qualitatively. If two objects are bound in an orbit with a SMA $a \leqslant a_{\text{merge}}$ the objects are deemed to be so tightly bound that they will merge no matter the path of the third object. To find the SMA of any binary orbit, we use the specific orbital energy equation:

$$E_{\text{binary}} = -\frac{\mu}{2a} \tag{55}$$

$$a = -\frac{\mu}{2E_{\text{binary}}} \tag{56}$$

with $\mu = GM$. The criteria thus reads:

$$a \leqslant \frac{a_0}{k} \tag{57}$$

$$E_{\text{Binary}} \geqslant -\frac{\mu k}{2a_0} \tag{58}$$

This will be our 3 Body merger criteria

This is, however, not the only outcome. The result can also produce a new binary with SMA $a > a_{\text{merger}}$ and a single object, unbounded from the binary and its constituents. As such we are want to determine the singlet for which $a_{\text{singlet}} < 0$ for all other objects. We can calculate these for the two binary constituents and for their center of mass. In order to make sure the singlet is truly unbound, we also impose that it must be further away from the binary than the initial singlet started $r_{\text{singlet}} > K \cdot a$ from our initial condition. Once we have ascertained that we have a new binary singlet state, we can use the formula for the merger time to determine if we will obtain a 2 body merger within the an interaction time as described earlier. We also include in our break condition one that does not allow for two objects to come arbitrarily close to one another. This is to prevent un-physical behaviour as our 2.5PN approximation will break down for small enough distances between our objects. As such we define the minimum distance as some multiple of the Schwarzschild radius:

$$r_{\text{min}} \equiv K r_{\text{sch}} = \frac{2KGM}{c^2} \tag{59}$$

This will be counted as a 3 body merger but turns out to be a very rare case.

As such the overall 3 body code will be executed As shown in figure (13):

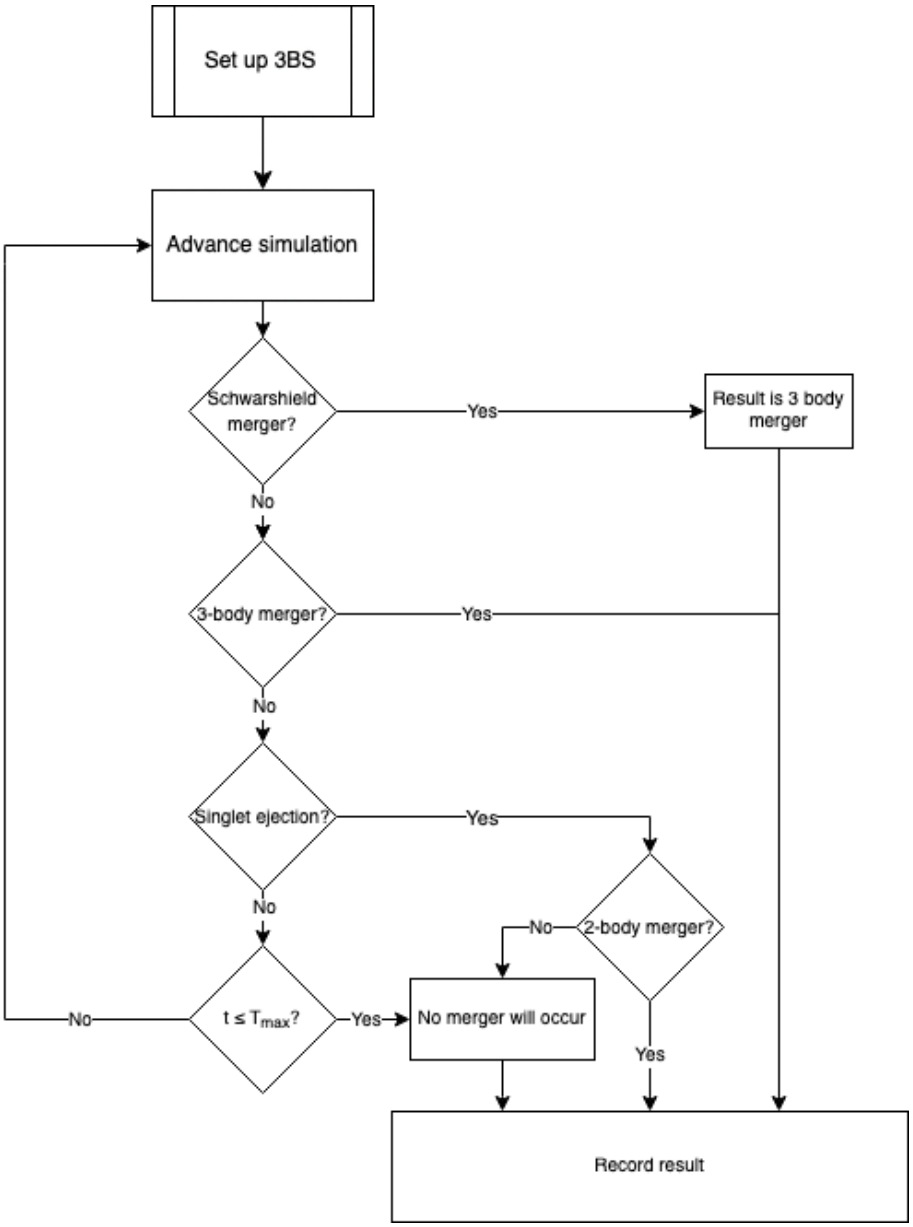

Figure 13: The overall flowchart. The individual criteria (Schwarshield merger, 2-body merger, 3-body merger) are functions with multiple criteria to be satisfied in order to return a positive result. The simulation itself does not execute these steps explicitly, as the `numpy.solve_ivp()` function can evaluate the time step and the criteria on its own through events.

4 Result

There are a number of choices that needs to be made for our simulation, which dictates initial setup and termination criteria. These criteria have been chosen based on qualitative analysis of choice simulations. As such the numerical results are subject to fluctuations dependent on the choices. For the rest of this document we will operate with the following choices.

- The scalar used to quantify the singlet initial radius in terms of the SMA is 5
- The scalar used to determine the cut-off for gravitational merger in terms of the the Schwarzschild radius is 10
- The scalar used to determine the cutoff for our conventional 3-body merger is $\frac{1}{10}$
- The number of temporary states has been qualitatively found to be 15.

At this point it also becomes necessary to express the initial energy of the 3-body system E_0. This is given as:

$$E_0 = \frac{1}{2}mv_s^2 - G\frac{2m^2}{r_s} + \frac{1}{2}\frac{m}{2}v_b^2 - G\frac{m^2}{r_b} \tag{60}$$

recalling our expression of the initial singlet energy as well as the speed of the binary we have:

$$E_0 = \frac{1}{2}m\left(v_\infty^2 + \frac{2G2m}{r_s}\right) - G\frac{2m^2}{r_s} + \frac{1}{2}\frac{m}{2}\frac{2Gm}{r_b} - G\frac{m^2}{r_b} \tag{61}$$

$$= \frac{1}{2}mv_\infty^2 - \frac{1}{2}\frac{Gm^2}{r_b} \tag{62}$$

4.1 Simulations

In order to verify the validity of the simulated results we started by testing cases for which we know the results. The results we obtained, while not completely in agreement with the established result, have proven sufficiently accurate within the range of interest.

4.1.1 2-Body simulations

We start by analysing 2 body motion and weather we see inspiral for circular orbits as well as circularisation for high eccentricity orbits. In order to verify this behaviour we utilise the vis-viva energy equation:

$$\epsilon = \frac{v^2}{2} - \frac{\mu}{r} = -\frac{1}{2}\frac{\mu^2}{h^2}(1-e^2) = -\frac{\mu}{2a} \tag{63}$$

to express the initial relative speed of our binary at variable eccentricities. We obtain:

$$v(t=0) = \sqrt{\frac{\mu}{r}(1-e)} \tag{64}$$

Where $\mu = GM$ and for initial conditions $r(t=0) = a$. From the same equation we can extract the eccentricity:

$$e = \sqrt{1 + \frac{2\epsilon h^2}{\mu^2}} \tag{65}$$

Where $h = |\mathbf{v} \times \mathbf{r}|$. The semi-major axis is found to be:

$$a = -\frac{\mu}{2\epsilon} \tag{66}$$

From earlier we have the theoretical framework for how the semi-major axis and eccentricity should evolve as a function of time.

As the 2 body system is deterministic, this simulation will not need a large sample size, and as such, figure (14) will provide an example of the inspiral as well as the semi-major axis obtained in relation to the theoretical behaviour.

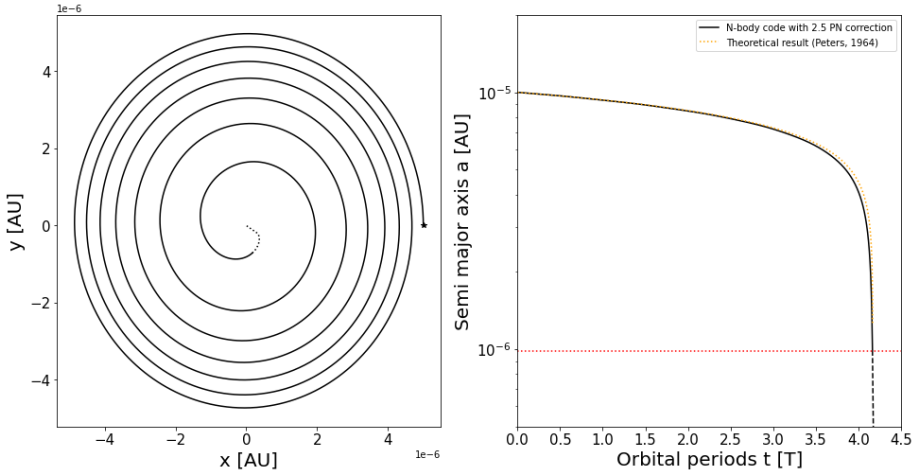

Figure 14: Inspiral for circular binary black hole. Left: The motion of one of the black hole during inspiral, note the dotted line at the center as we cross the Schwarshield at which point the behaviour of the inspiral becomes non-physical. Right: The SMA plotted as a function of time with the theoretical behaviour plotted in dotted orange. The red dotted line at the bottom is the Schwarshield radius.

As can be seen we have general agreement between theoretical and numerical result. Note here that we have chosen a sufficiently small initial distance a_0 such that inspiral occurs within just a few orbital periods. Furthermore, the

simulation also breaks down for sufficiently small distances $\Delta r < r_{sch}$, which can be seen by the non-physical behaviour marked in dotted line at the end of the inspiral. This will, however, not become a problem as our termination criteria are set well before such behaviour should occur.

For the high eccentricity limit $e \approx 1$ we have that the separation distance becomes rather important in order to obtain the theoretical behaviour. Furthermore there is a tendency for the simulation to exhibit quite un-physical behaviour as the inspiral circularises the orbit. As can be seen below there comes a point where the orbit seems to rapidly eccentrify again while the SMA keeps shrinking. This is a problem that has not been rectified for the rest of the project but could prove a source for errors. It will however not be a problem for the initial setup of our orbits as the binary will be circular. We can also see that the simulated eccentricity oscillates while following the rough theoretical path. These oscillations seem to increase as the orbit circularises and has been attested to in [3]

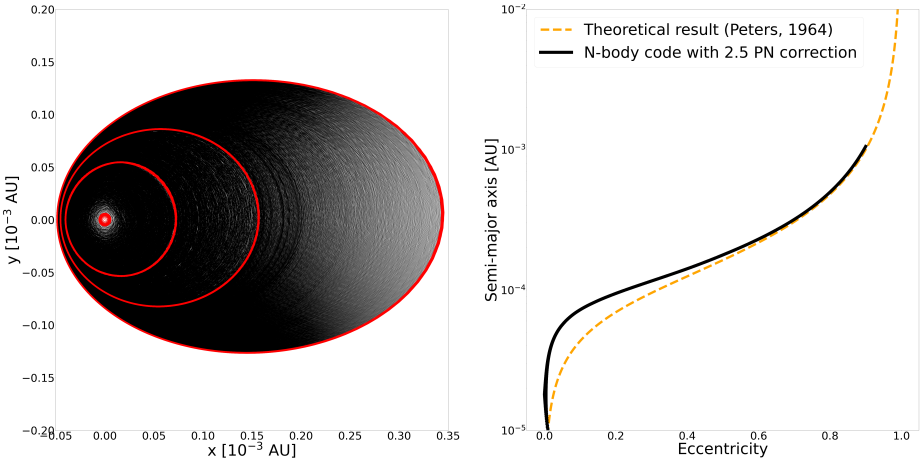

Figure 15: Inspiral for highly eccentric black hole binary. Left: The movement of one of the black holes during inspiral. Due to the number of orbits needed for inspiral and circularisation regions have been plotted in red to show the progress for a few orbits and to note the gradual inspiral and circularisation experienced by the black hole. Right: The SMA plotted as a funtion of eccentricity with the theoretical distribution plotted as the orange dotted line. Note the initial adherance to the theoretical behaviour until about $e = 0.4$ where the simulation starts to diverged, but around $e = 0$ the simulation rapidly returns to the theory. The oscillation around $e = 0$ is the result of the limitations of the integration scheme. It can also be seen that at $SMA = 10^{-5}$ AU the eccentricity seems to slowly rise again. This was a problem I was not able to explain but it did not seem to skew the results in the end.

4.1.2 3-Body simulations

For the 3-body system, we utilise the `solve.ivp()` function to evaluate the termination criterion through events. These are conditions set up so that when the condition value changes parity, the event is recorded and the code terminates.

As such our termination criterion has to be formulated as step-functions and for those with multiple parameters reaching certain values, their step-function transforms has to be summed. Below are the the events as written in the code:

```
    def relativePVfunction(Yin_arr):
        Yin_nrobj_posvel    = np.reshape(Yin_arr,(nr_obj,6))
        pos_ij = np.zeros([nr_obj,3]) # Setup the array for
                                        position difference ij
        vel_ij = np.zeros([nr_obj,3]) # Setup the array for
                                        velocity difference ij
        r_ij = np.zeros([1,nr_obj]) # Setup the array for distance
                                        ij
        v_ij = np.zeros([1,nr_obj]) # Setup the array for speed
                                        difference ij


        for i in range(nr_obj):
            j0 = np.mod(i,nr_obj)
            j1 = np.mod(i+1,nr_obj)
            j2 = np.mod(i+2,nr_obj)
            pos_ij[j0,:] = Yin_nrobj_posvel[j1,:3]-Yin_nrobj_posvel
                                            [j2,:3] # computing
                                            the relative position
                                             using numpys modular
                                             function to avoid
                                            repeats

            vel_ij[j0,:] = Yin_nrobj_posvel[j1,3:]-Yin_nrobj_posvel
                                            [j2,3:] # computing
                                            the relative velocity
                                             using numpys modular
                                             function to avoid
                                            repeats
        r_ij = np.sqrt(np.sum(pos_ij**2,axis = 1)) #calculating the
                                            distance
        v_ij = np.sqrt(np.sum(vel_ij**2,axis = 1)) #calculating the
                                            speed difference
        return pos_ij, vel_ij, r_ij, v_ij

    def SchwarzschildMerger(t,Yin_arr): # input are time, position
                                        and velocity
        __,__,r_ij,__ = relativePVfunction(Yin_arr) #calling the PV
                                            function to obtain the
                                            distance

        return r_ij.min() - 10*PN_gamma*2*M #return the difference
                                            between the smallest
                                            distance and the scaled
                                            Schwarzschild radius
```

Note that the `relativePVfunction()` function will be used for the other events as well but will not be explicitly written.

```
def  Ejection(t,Yin_arr): # input are time, position and
                                velocity
    pos_ij,vel_ij,r_ij,v_ij = relativePVfunction(Yin_arr) #
                                    calling the PV function
                                    to obtain all desired
                                    values

    pos_com = np.zeros([nr_obj,3])
    vel_com = np.zeros([nr_obj,3])
    r_com = np.zeros(nr_obj)
    v_com = np.zeros(nr_obj)

    # The loop below calculates the COM
    #relative speed and distance of each binary
    #in relation to the third object for
    #each of the three configurations of binary and singlet

    for i in range(nr_obj):
        j1 = np.mod(i+1,nr_obj)
        j2 = np.mod(i+2,nr_obj)
        pos_com = 0.5 *(pos_ij[j1,:]+pos_ij[j2,:])
        r_com[i] = np.sqrt(np.sum(pos_com**2, axis = 0))
        vel_com = 0.5 *(vel_ij[j1,:]+vel_ij[j2,:])
        v_com[i] = np.sqrt(np.sum(vel_com**2,axis = 0))

    # The COM energy and SMA is calculated relative to the
                                    singlet

    E_com = 1/2 * v_com**2 - 3*M/r_com
    sma_com = -3*M/(2*E_com)

    r_mask = (r_com == max(r_com)) # The greatest distance
                                    between binary and
                                    singlet is found


    # Below the criterion for the separation of the binary
    # and the singlet is greater than 10 the initial distance
    #between singlet and binary as well as the singlet being
    #unbound gravitationally from the singlet
    r_value = np.heaviside(10*scalefactor*SMA_bin-r_com[r_mask]
                                    ,0)
    a_value = np.heaviside(sma_com[r_mask],0)

    return  a_value + r_value
```

The 2-Body merger criterion will only be checked for once an ejection has occurred and as such it is not an event in and of itself.

```
def BodyMerger2(Result,Yin_arr):
    if (Result == 3): # 3 is the tag given to ejection cases
        pos_ij,vel_ij,r_ij,v_ij = relativePVfunction(Yin_arr[:,
                                        -1]) # Calling the PV
                                         function

        com_arg = np.where(r_ij == r_ij.min()) #find the
                                        closest pair

        # Below we calculate the merger time of the bound
                                        binary post ejection
        eps = v_ij[com_arg]**2/2 - mass_binary/r_ij[com_arg]
        h = vel_ij[com_arg,0]*pos_ij[com_arg,1]-vel_ij[com_arg,
                                        1]*pos_ij[com_arg,0]

        e = np.sqrt(1+(2*eps*(h**2))/(mass_binary**2))
        a = -mass_binary/(2*eps)
        merger_time = 5/512 * (a**4)/((0.5*mass_binary)**3) * (
                                        1-(e**2))**(7/2)

        # The cutoff merger time is converted to code units
        T_GW = (c_SI**5/G_new_SI**3 * AU_SI**4 / M_sun_SI**3)/(
                                        sec_year) *
                                        merger_time
        # Checking weather the merger time is less than the
                                        cutoff merger time
        if (T_GW < 10**5):
            return Result+1 # 2-Body mergers are tagged as 4
        else:
            return Result
    else:
        return Result
```

```
def BodyMerger3(t,Yin_arr):
    __,__,r_ij,v_ij = relativePVfunction(Yin_arr) # Calling the
                                         PV function
    E_ij = 1/2 * v_ij**2 - m_bin/r_ij # Calculating the
                                        specific energy of each
                                        binary
    sma_ij = -m_bin/(2*E_ij) # Calculating the SMA of each
                                        binary

    r_mask = (r_ij == min(r_ij)) #find the two BHs closest to
                                        each other
    # The value below is to make sure the binary is in fact
                                        bound as the value will
                                        be >0 for an unbound pair
    sma_min = np.heaviside(-sma_ij[r_mask],0)
    # The value below is to check if the SMA is smaller than
                                        the desired SMA
    sma_max = np.heaviside(sma_ij[r_mask]-SMA_bin/10,0)
    # The conditions are added together and if both are true
                                        the returned value is 0
    return sma_min + sma_max
```

To not skew our results, we furthermore made sure to rotate the binary by

some uniform random rotation. From this we ran 10000 simulations for each chosen semi major axis. The result of this can be seen below:

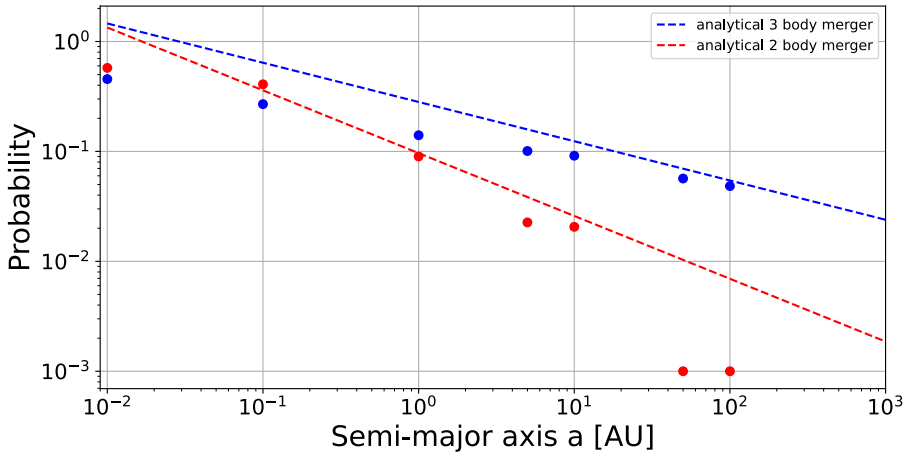

Figure 16: Merger probabilities for 3- and 2-body mergers at different initial SMA. Note the asymptotic behaviour of the 3-body merger as it approaches the theoretical distribution. The explanation for this is twofold and caused by prompt ejections of the singlet which is not accounted for theoretically as well as the assumption that the probability can be written as a sum of individual interactions. The 2-body merger diverges for sufficiently high SMA, which is most likely due to the low amount of 2-body mergers at that scale, leading to a high spread. While not included here, earlier simulations performed during this project does show a spread, yet general adherance to the theoretical distributions.

As can be seen from the distribution, we have certain incongruities: The 3-body merger probability only approaches the theoretical distribution for $a > 10^2$ AU. This is not unexpected and has at least two explanations: In order for the 3-body merger to occur it becomes necessary to enter a resonant state where the singlet is not promptly ejected, which for smaller a becomes less likely. Secondly when the theoretical distribution was derived we made the assumption that it could be written out as a sum of uncorrelated merger probabilities. This assumption of independence does, however, break down for small a when p_3 approaches unity. The 2-body merger distribution seems to have a divergent behaviour for $a < 10$ AU. This is very likely due to the low amount of captures expected at large SMA. The statistical uncertainty will naturally grow as the merger probability falls. This has also been observed throughout the project as earlier merger probabilities have been derived which had much higher simulated 2 merger probabilities for large SMA.

Having verified the general behaviour of the 2- and 3-body system is in accordance with expected theoretical results, we can move on to the 3 body interactions generally.

4.1.3 SMBH integration

For the SMBH implementation we added a 10^9 solar mass black hole and positioned the 3-body system at some scalar distance of the tidal radius. We orient the 3-body system by some uniformly random rotation relative to the SMBH. The termination criterion are the same as before. Running 10000 simulations for different tidal radii we obtain the following distribution.

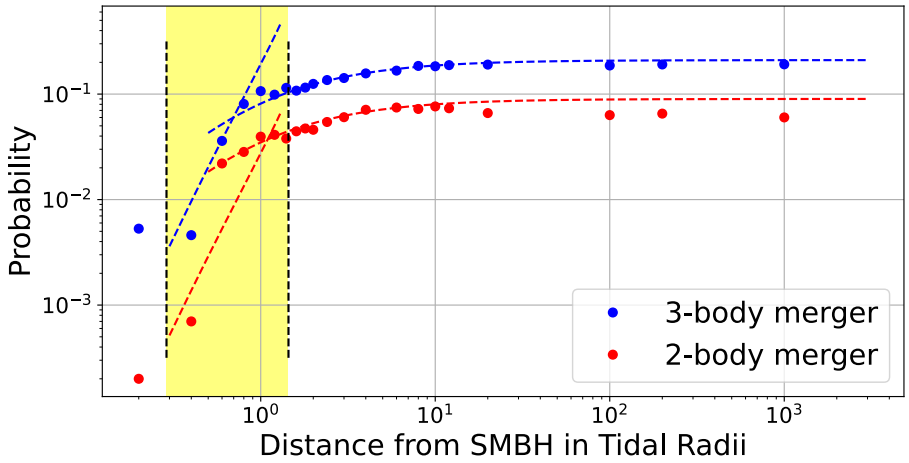

Figure 17: Probability distribution for mergers as a function of SMBH separation in terms of tidal radii. The yellow zone is the near region while to the right is the far region and the left, the completely unstable region. We see that for the 3-body merger we see that when we enter the near region the result starts to deviate from the far region distribution and starts to follow the near region distribution as expected. For the 2-body merger we see that it follows the far region through almost the entire near region and only at $r_{hill} \approx a$ we see that it approaches the near region distribution. The reason for this is because the near region distribution was made for multiple semi ejections but for the 2-body merger that need not be the case. A single interaction between the binary and the singlet before ejection could disturb the binary to the point of inspiral within the cut-off time.

As can be seen we have a general agreement with the theoretical distribution for tidal scalars $n > 1$ as would be expected. The reason our distributions veer off for smaller n is most likely due to the indifference to rotation of the 3-body system. At this scale our geometric distributions should take over, which it does for the 3-body merger rate, but not for the 2-body case. Here we see an adherence to the other distribution for a much longer time. The explanation for this is that while the 3-body merger rate depends on the singlet interacting with the binary, the 2-body need not be so dependent. Here a single interaction before ejection could be enough to let the inspiral happen within an interaction time. As such we only see the divergence when the hill radius $r_{\text{Hill}} \approx a$. It is also important to note that for this distribution the fitting parameter k has been found to be$k \approx 10^5$. This does have some unfortunate implications as we defined $r_s = k \cdot R$ and would make the binary distance much greater than the

SMBH distance. This indicates that the assumption made on how to relate r_s and R is faulty. This implies that another assumption might be needed instead, as the resulting distributions seem to follow the data remarkably well otherwise.

From fig. (18) below we can see that while the ejections criterion in the code, shown in the COM does not always appear to be justified, as it appears they could still re-merge, the SMBH frame makes their departure evident.

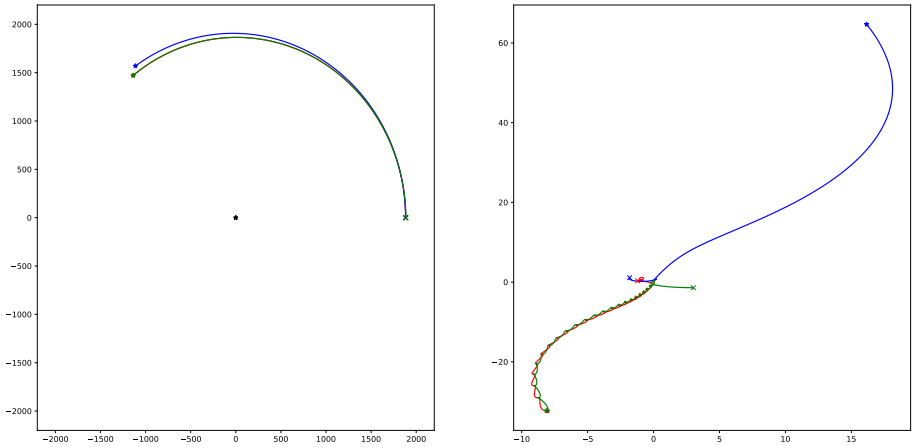

Figure 18: The ejection of a singlet from 3-body interactions in the presence of a SMBH. The SMBH is at a distance of 2 tidal radiis and the SMA is 1 AU. Note the binary and singlet are at a clear distance compared to the binary's internal distance.

Below can be seen the impact of the SMBH on a particular 3-body system. The rotation between the singlet and binary is kept constant and the impact parameter is scaled similarly for each of the different simulations. Each row shows a different distance from the SMBH to the 3-body system with row one being the vacuum case at infinite distance to the SMBH while the second to sixth row get progressively closer to the SMBH, in terms of tidal radii. The columns represent different binary SMA. For the SMBH simulations the rotation of the 3-body system is such that the singlet is on the far side of the binary. The result of each simulation is shown in the title of each plot. As can be seen we see a lot more ejections as we move closer to the SMBH and when the SMA becomes larger. This is consistent with our distributions and theoretical framework.

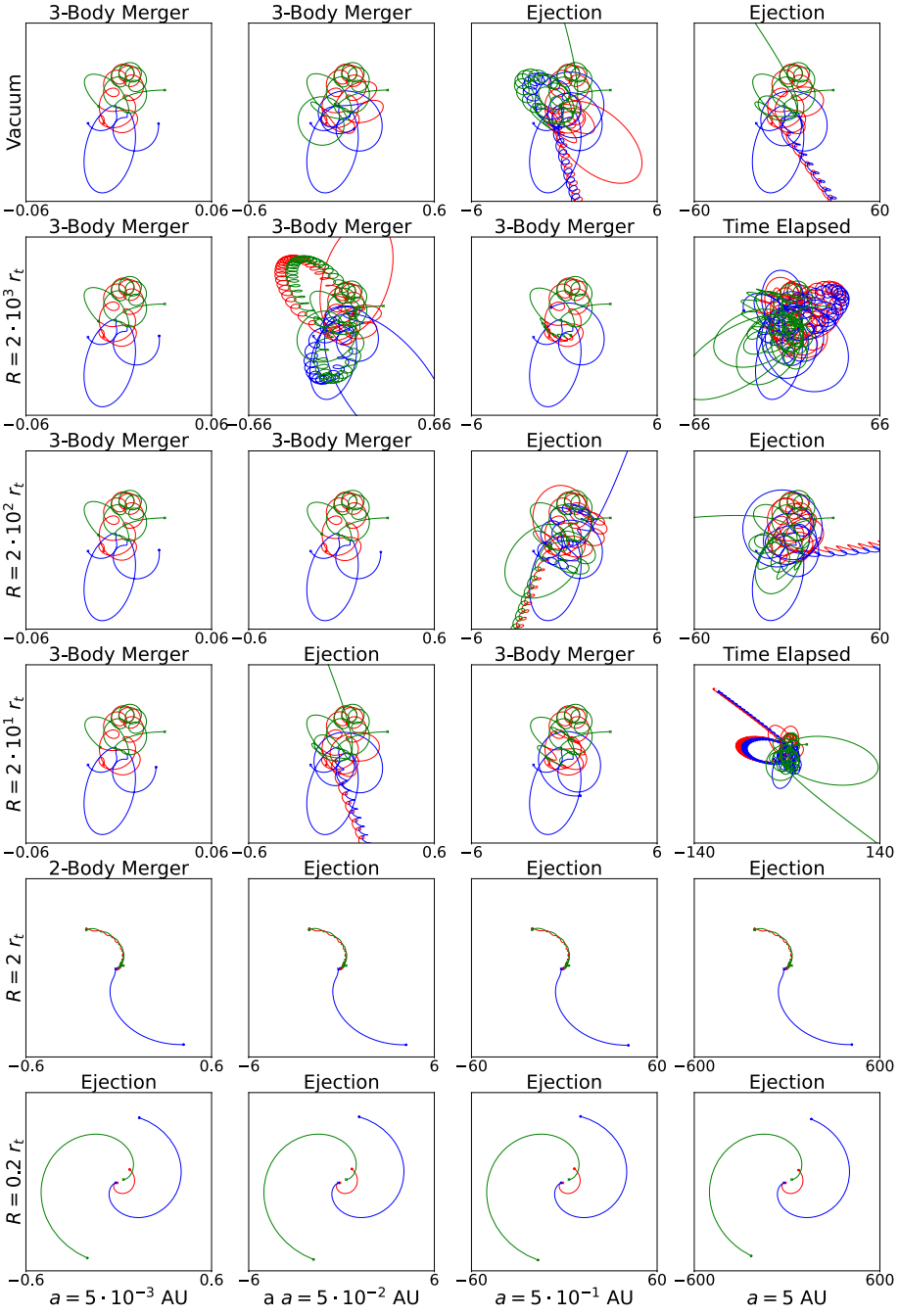

Figure 19: Comparison between 3-body interaction. Each row is a different separation to the SMBH with the top being the Vacuum 3-body system, second row being at 2000 tidal radii, third row being 200, fourth being 20, fifth being 2, and sixth being 0.2 tidal radii. Each column is a different SMA: First column is 0.005 AU, second being 0.05, third being 0.5, and fourth being 5 AU. The scale of each plot is in AU as well and the extend of each is shown in the bottom. The result of each simulation is shown in the title.

5 Discussion

While the results presented so far are promising, they obviously diverge from the analytical solutions in different aspects. In this section we will go through these inconsistencies and try to analyse their impact on the final result and the validity of any conclusions drawn from this.

The 2-body simulation showed a discrepancy between the theoretical high eccentricity behaviour and the numerical behaviour. As explained, this is not fully understood but might be a facet of the numerical choices made in the simulation. As the numerical solution seemed to show the circularisation through inspiral to a point, this was generally deemed sufficiently accurate to proceed, but the cause has not been determined at time of writing.

There is a number of different aspects of the termination criteria choices that could be improved upon. The choices made where based on qualitative trial and error as well as a priori assumptions. The choices of these could be refined and their cut-off values could be chosen through a more rigorous parameter optimisation. This, however does not seem to be the biggest detractor from the general validity of the results, since the effects of the choices only seemed to have affected the 2-body merger in the original 3-body simulations. The impact seem to have been that only 1/3 of the expected 2-body mergers seem to have occurred while the trajectory of the probability as a function of SMA seem to have been accurate.

The assumption of uniform rotation of the 3-body system with respect to the SMBH is of course problematic when the SMBH separation becomes sufficiently small. When $R \ll r_3$ constraints should be put on the 3-body rotational angle as it would not be possible for a singlet to approach from certain angles. This, however has already largely been accounted for by the geometric probability factor.

The termination criterion for the SMBH are the same as before, which could pose a problem with a singlet ejected, which under normal circumstances would never return, being able to intercept the new binary at some later point due to still orbiting the SMBH. This assumes, however, that only our three bodies orbit the SMBH. In Practice due to the real environment of an AGN, the time it would take these objects to meet again is much greater than the relaxation time of the AGN objects. As such, when they meet again they will not retain any information of their previous encounter.

6 Conclusion

In this thesis we set out to analyse the possibility of active galactic nuclei as producers of black hole mergers as posited by Samsing and D'Orazio [8]. This, we did by focusing on stable binaries, with separation distances to great for gravitational inspiral within a Hubble time, disturbed by close interaction with a third single black hole. First we verified, through simulations, the possibility of such a 3-body system to be a probable source, with numerical results match-

ing the theoretical probability distributions, with some restrictions. From here we showed that introducing the environment of a SMBH at some separation distance R to the 3-body system, did affect the probability but did so only for sufficiently small R. For distances resulting in stable 3-body initial setup ($r_{\text{Hill}} \gtrsim r_3$) the simulation seemed to confirm the theoretical distribution, and reducing to the simple 3-body system for large separations ($R \to \infty$).

This is of course only a simplified model and as such a lot of further mechanics needs to be implemented to verify the validity in the future. One notable simplification is the absence of an accretion disk which would provide some electrohydrodynamic component to the final probability distribution.

While there are many aspects of the results in this thesis which need further investigation and optimisation, the results seem to support AGN as a factory for black hole mergers.

A Code

Below is the entire code used in the simulations. Note that it output the outcome of the 3-body interactions as a value between 0 and 4 as well as the time and position and velocity of the 3 black holes. The simulations are made with the `solve.ivp()` function. Earlier `odeint()` was due to issues when the SMBH was implemented the numerical solver was updated.

```
from matplotlib import pyplot as plt
import numpy as np
from scipy.integrate import odeint , solve_ivp
import datetime as dat
import os
from tqdm import trange
# from matplotlib.gridspec import GridSpec
# from body_merger import*

#Units and conversions:

#code units: Rsun, Msun, G=1, ...
c_SI        = 299792458.0

                                    #m/s
M_sun_SI    = 1.989*(10.**30.)

                                    #kg
R_sun_SI    = 695800000.

                                    #m
AU_SI       = 149597871000.

                                    #m
G_new_SI    = 6.67*(10.**(-11.))

                                    #Nm2/kg-2
T_SI = np.sqrt(AU_SI**3/(G_new_SI*M_sun_SI))

                                    #Period time in SI units

AU_U        = AU_SI/R_sun_SI

                                    #from dist AU to code units (U)



kmsec_U     = 1000./np.sqrt(G_new_SI*M_sun_SI/R_sun_SI)
                                                        #from vel
                                    km/sec to code units (U)
sec_year    = 31536000.
m_parsec    = 3.086*(10**16.)

                                    #m
PN_gamma    = 9.86719698246e-09

                                    #G_new_SI*M_sun_SI/(AU_SI*c_SI**2
```

```
                                    ) useful for swarschild radius

#Functions:



def relativePVfunction(Yin_arr):
        Yin_nrobj_posvel    = np.reshape(Yin_arr,(nr_obj,6))
        pos_ij = np.zeros([nr_obj,3]) # Setup the array for
                                        position difference ij
        vel_ij = np.zeros([nr_obj,3]) # Setup the array for
                                        velocity difference ij
        r_ij = np.zeros([1,nr_obj]) # Setup the array for distance
                                        ij
        v_ij = np.zeros([1,nr_obj]) # Setup the array for speed
                                        difference ij


        for i in range(nr_obj):
            j0 = np.mod(i,nr_obj)
            j1 = np.mod(i+1,nr_obj)
            j2 = np.mod(i+2,nr_obj)
            pos_ij[j0,:] = Yin_nrobj_posvel[j1,:3]-Yin_nrobj_posvel
                                            [j2,:3] # computing
                                            the relative position
                                             using numpys modular
                                             function to avoid
                                            repeats

            vel_ij[j0,:] = Yin_nrobj_posvel[j1,3:]-Yin_nrobj_posvel
                                            [j2,3:] # computing
                                            the relative velocity
                                             using numpys modular
                                             function to avoid
                                            repeats
        r_ij = np.sqrt(np.sum(pos_ij**2,axis = 1)) #calculating the
                                        distance
        v_ij = np.sqrt(np.sum(vel_ij**2,axis = 1)) #calculating the
                                        speed difference
        return pos_ij, vel_ij, r_ij, v_ij


def merger(RVA_param):
    r_ij = RVA_param[2]
    v_ij = RVA_param[3]

    E_ij = 1/2 * v_ij**2 - m_bin/r_ij
    asma_ij = -m_bin/(2*E_ij)
    return (asma_ij), (E_ij)



def func_v_esc(RVA_param):
    pos_ij = RVA_param[0]
    vel_ij = RVA_param[1]
    r_ij = RVA_param[2]
```

```
    pos_com = np.zeros([nr_obj,3])
    vel_com = np.zeros([nr_obj,3])
    vel_com_align = np.zeros((1,nr_obj),dtype = 'd')
    vel_align = np.zeros((1,nr_obj),dtype = 'd')


    for i in range(nr_obj):
        pos_com[np.mod(i,nr_obj),:] = 0.5*(pos_ij[np.mod(i+1,nr_obj
                                           ),:]-pos_ij[np.mod(i+2,
                                           nr_obj),:])
        vel_com[np.mod(i,nr_obj),:] = 0.5*(vel_ij[np.mod(i+1,nr_obj
                                           ),:]-vel_ij[np.mod(i+2,
                                           nr_obj),:])

    vel_com_align = np.sum(vel_ij*pos_ij,axis = 1)/r_ij
    v_esc_com = np.sqrt(2*m_bin/r_ij)


    r_com = np.sqrt(np.sum(pos_com**2,axis = 1))

    v_esc = np.sqrt(6*M/r_com)

    vel_align = np.sum(vel_com*pos_com,axis = 1)/r_com

    v_norm_esc = vel_align/v_esc
    v_norm_com_esc = vel_com_align/v_esc_com

    return abs(v_norm_esc), abs(v_norm_com_esc), r_com

def merger_time(RVA,m_bin,argument):

    pos = RVA[0]
    vel = RVA[1]
    r = RVA[2]
    v = RVA[3]
    # print(pos,vel,r,v)

    eps = v[argument]**2/2 - m_bin/r[argument]
    h = vel[argument,0]*pos[argument,1]-vel[argument,1]*pos[
                                        argument,0]

    e = np.sqrt(1+(2*eps*(h**2))/(m_bin**2))
    a = -m_bin/(2*eps)

    return 5/512 * (a**4)/((0.5*m_bin)**3) * (1-(e**2))**(7/2)

def rot(x,t):
    y = np.zeros(len(x))
    R = np.array([[np.cos(t),np.sin(t),0],[-np.sin(t),np.cos(t),0],
                                        [0,0,1]])
    y = x.dot(R)
    return y

def func_dt(RVA_param):     #incl masses later on
    #reshape:
    dt_fac              = 1e10
```

```
    dt_min              = 0
    pos_ij = RVA_param[0]
    r_ij = RVA_param[2]
    v_ij = RVA_param[3]
    a_ij = np.sqrt(np.sum(((M/(r_ij.reshape(nr_obj,1)**2.))*(pos_ij
                                    /r_ij.reshape(nr_obj,1)))**2,
                                    axis = 1))
    dt_rvra     = np.append(r_ij/v_ij, np.sqrt(r_ij/a_ij))
    # print(dt_rvra)
    min_dt_rvra = min(dt_rvra)

    if (min_dt_rvra<=dt_fac):
        dt_fac = min_dt_rvra
        # print(dt_fac)
    if (min_dt_rvra <= dt_min):
        dt_fac = dt_min
        # print('this should work yes?',dt_fac)

    return dt_fac


def Init_condition(SMA,m0,Y0):
    #Set b1 and b2 up in a CIRCULAR binary with COM in (0,0,0):
    theta                   = np.random.uniform(0,2*np.pi)


    v_redmass               = np.sqrt(m_bin/SMA)


    if (ROT_bool== True):
        b1_posxyz_binCM     = rot(np.array([ (m0[1]/m_bin)*SMA,0,0]
                                    ,dtype=object),theta)
        b2_posxyz_binCM     = rot(np.array([-(m0[0]/m_bin)*SMA,0,0]
                                    ,dtype=object),theta)
        b1_velxyz_binCM     = rot(np.array([0, (m0[1]/m_bin)*
                                    v_redmass,0],dtype=object
                                    ),theta)
        b2_velxyz_binCM     = rot(np.array([0,-(m0[0]/m_bin)*
                                    v_redmass,0],dtype=object
                                    ),theta)
    else:
        b1_posxyz_binCM     = np.array([ (m0[1]/m_bin)*SMA,0,0],
                                    dtype=object)
        b2_posxyz_binCM     = np.array([-(m0[0]/m_bin)*SMA,0,0],
                                    dtype=object)
        b1_velxyz_binCM     = np.array([0, (m0[1]/m_bin)*v_redmass,
                                    0],dtype=object)
        b2_velxyz_binCM     = np.array([0,-(m0[0]/m_bin)*v_redmass,
                                    0],dtype=object)


    r_max = SMA
    b_theoretical = r_max*np.sqrt(1+2*m_bin/(v_inf**2 * r_max))

    b_inf = b_theoretical*np.random.uniform(-1,1)
    r_sim = scalefactor*SMA
    b_sim                   = b_inf/np.sqrt(1+2*m_bin/(v_inf**2 *
```

```
                                        r_sim))

    v_sim                   = v_inf*b_inf/b_sim
    r_x                     = np.sqrt(r_sim**2-b_sim**2)

    #IC for b3:

    if (nr_obj == 3):
        b3_posxyz_binCM     = np.array([r_x,b_sim,0],dtype=object)
        b3_velxyz_binCM     = np.array([-v_sim,0,0],dtype=object)
    if(SMBH_bool== True):
        b1_posxyz_binCM = b1_posxyz_binCM + r_tidal
        b2_posxyz_binCM = b2_posxyz_binCM + r_tidal
        if (nr_obj == 3):
            b3_posxyz_binCM = b3_posxyz_binCM + r_tidal

        b1_velxyz_binCM = b1_velxyz_binCM + v_tidal
        b2_velxyz_binCM = b2_velxyz_binCM + v_tidal
        if (nr_obj == 3):
            b3_velxyz_binCM = b3_velxyz_binCM + v_tidal


    Y0[0*6:0*6 + 6]     = np.append(b1_posxyz_binCM,
                                    b1_velxyz_binCM)
    Y0[1*6:1*6 + 6]     = np.append(b2_posxyz_binCM,
                                    b2_velxyz_binCM)
    if (nr_obj == 3):
        Y0[2*6:2*6 + 6]     = np.append(b3_posxyz_binCM,
                                       b3_velxyz_binCM)

    return Y0

def func_NBODY_Ydot(t, Yin_arr):    #incl masses later on
    #reshape:
    Yin_nrobj_posvel    = np.reshape(Yin_arr,(nr_obj,6))
    #define:
    Ydot_nrobj_posvel   = np.zeros((nr_obj,6), dtype='d')

    for i in range(0,nr_obj):
        a_ij_tot    = np.array([0,0,0])
        pos_i       = Yin_nrobj_posvel[i,0:3]
        vel_i       = Yin_nrobj_posvel[i,3:6]

        for j in range(0,nr_obj):
            if (i != j):
                mi      = m0_arr[i] #
                mj      = m0_arr[j] #
                pos_j   = Yin_nrobj_posvel[j,0:3]
                vel_j   = Yin_nrobj_posvel[j,3:6]
                pos_ij  = pos_j - pos_i
                vel_ij  = vel_j - vel_i
                #print np.sqrt(np.sum(pos_ij[:]**2.)), i,j
                r_ij    = np.sqrt(np.sum(pos_ij**2.))
                v_ij    = np.sqrt(np.sum(vel_ij**2.))
                #Newtonian acc:
                acc_ij        = (mj/(r_ij**2.))*(pos_ij/r_ij)
                #2.5PN acc:
```

```
                n_ij = pos_ij/r_ij
                n_dot_vi = np.dot(n_ij,vel_i) #
                n_dot_vj = np.dot(n_ij,vel_j) #
                a25_ij      = -(PN_gamma**(5./2.))*(4./5.)*(mi*mj/(
                                                    r_ij**3))*(vel_ij
                                                    *(-(v_ij**2.) + 2
                                                    .*(mi/r_ij) - 8.*
                                                    (mj/r_ij)) + n_ij
                                                    *(n_dot_vi-
                                                    n_dot_vj)*(3.*(
                                                    v_ij**2.) - 6.*(
                                                    mi/r_ij) + (52./3
                                                    .)*(mj/r_ij)))
                #total acc:
                a_ij_tot    = a_ij_tot + acc_ij + a25_ij
                # print(np.dot(-pos_i,a_ij_tot))



        if(SMBH_bool == True):
            pos_jSMBH = pos_SMBH-Yin_nrobj_posvel[i,0:3]
            r_jSMBH = np.sqrt(np.sum(pos_jSMBH**2.))

            a_jSMBH = (M_SMBH/(r_jSMBH**2))*(pos_jSMBH/r_jSMBH)

            a_i_tot = a_ij_tot + a_jSMBH
        else:
            a_i_tot = a_ij_tot



        Ydot_nrobj_posvel[i,0:3]    = np.ravel(vel_i)
        Ydot_nrobj_posvel[i,3:6]    = np.ravel(a_i_tot)
    Yout_arr    = np.ravel(Ydot_nrobj_posvel)
    return Yout_arr


def SchwarzschildMerger(t,Yin_arr): # input are time, position and
                                    velocity
        __,__,r_ij,__ = relativePVfunction(Yin_arr) #calling the PV
                                         function to obtain the
                                        distance

        return r_ij.min() - 10*PN_gamma*2*M #return the difference
                                        between the smallest
                                        distance and the scaled
                                        Schwarzschild radius



def BodyMerger3(t,Yin_arr):

        __,__,r_ij,v_ij = relativePVfunction(Yin_arr) # Calling the
                                         PV function
        E_ij = 1/2 * v_ij**2 - m_bin/r_ij # Calculating the
                                        specific energy of each
```

```
                                        binary
        sma_ij = -m_bin/(2*E_ij) # Calculating the SMA of each
                                        binary

        r_mask = (r_ij == min(r_ij)) #find the two BHs closest to
                                        each other
        # The value below is to make sure the binary is in fact
                                        bound as the value will
                                        be >0 for an unbound pair
        sma_min = np.heaviside(-sma_ij[r_mask],0)
        # The value below is to check if the SMA is smaller than
                                        the desired SMA
        sma_max = np.heaviside(sma_ij[r_mask]-SMA_bin/10,0)
        # The conditions are added together and if both are true
                                        the returned value is 0
        return sma_min + sma_max



def  Ejection(t,Yin_arr): # input are time, position and velocity
        pos_ij,vel_ij,r_ij,v_ij = relativePVfunction(Yin_arr) #
                                        calling the PV function
                                        to obtain all desired
                                        values


        pos_com = np.zeros([nr_obj,3])
        vel_com = np.zeros([nr_obj,3])
        r_com = np.zeros(nr_obj)
        v_com = np.zeros(nr_obj)

        # The loop below calculates the COM
        #relative speed and distance of each binary
        #in relation to the third object for
        #each of the three configurations of binary and singlet

        for i in range(nr_obj):

            j1 = np.mod(i+1,nr_obj)
            j2 = np.mod(i+2,nr_obj)
            pos_com = 0.5 *(pos_ij[j1,:]+pos_ij[j2,:])
            r_com[i] = np.sqrt(np.sum(pos_com**2, axis = 0))
            vel_com = 0.5 *(vel_ij[j1,:]+vel_ij[j2,:])
            v_com[i] = np.sqrt(np.sum(vel_com**2,axis = 0))

        # The COM energy and SMA is calculated relative to the
                                        singlet

        E_com = 1/2 * v_com**2 - 3*M/r_com
        sma_com = -3*M/(2*E_com)

        r_mask = (r_com == max(r_com)) # The greatest distance
                                        between binary and
                                        singlet is found

        # Below the criterion for the separation of the binary
        # and the singlet is greater than 10 the initial distance
```

```
        #between singlet and binary as well as the singlet being
        #unbound gravitationally from the singlet

        r_value = np.heaviside(10*scalefactor*SMA_bin-r_com[r_mask]
                                            ,0)
        a_value = np.heaviside(sma_com[r_mask],0)

        return  a_value + r_value

def  Ejectiona(t,Yin_arr):
    RVA_parameter = relativePVfunction(Yin_arr)
    v_tot, v_com_tot, r_com = func_v_esc(RVA_parameter)

    r_mask = (r_com == max(r_com))
    r_value = np.heaviside(2*scalefactor*SMA_bin-r_com[r_mask],0)
    v_value = np.heaviside(1-v_tot[r_mask],0)
    c_value = np.heaviside(v_com_tot[r_mask]-1,0)
    # print(r_com[r_mask],v_tot[r_mask],v_com_tot[r_mask])

    return  r_value + v_value + c_value

def BodyMerger2(Result,Yin_arr):
    if (Result == 3): # 3 is the tag given to ejection cases
        pos_ij,vel_ij,r_ij,v_ij = relativePVfunction(Yin_arr[:,-1])
                                            # Calling the PV
                                            function

        com_arg = np.where(r_ij == r_ij.min()) #find the closest
                                            pair

        # Below we calculate the merger time of the bound binary
                                            post ejection
        eps = v_ij[com_arg]**2/2 - m_bin/r_ij[com_arg]
        h = vel_ij[com_arg,0]*pos_ij[com_arg,1]-vel_ij[com_arg,1]*
                                            pos_ij[com_arg,0]

        e = np.sqrt(1+(2*eps*(h**2))/(m_bin**2))
        a = -m_bin/(2*eps)
        merger_time = 5/512 * (a**4)/((0.5*m_bin)**3) * (1-(e**2))
                                            **(7/2)

        # The cutoff merger time is converted to code units
        T_GW = (c_SI**5/G_new_SI**3 * AU_SI**4 / M_sun_SI**3)/(
                                            sec_year) * merger_time
        # Checking weather the merger time is less than the cutoff
                                            merger time
        if (T_GW < 10**5):
            return Result+1 # 2-Body mergers are tagged as 4
        else:
            return Result
    else:
        return Result


#Below the events are set to terminate the simulation if they are
                                    fulfilled.
#Furthermore the ejection and three body merger are set to only
```

```
                                    accept
#going from positive to negative values

SchwarzschildMerger.terminal = True
BodyMerger3.terminal = True
BodyMerger3.direction = -1
Ejection.terminal = True
Ejectiona.terminal = True
Ejection.direction = -1


#Boolean parameters
Save_val = True
SMBH_bool = False
print_result = True
ROT_bool = False


nr_obj  = 3             #number of objects
dt_scale    = 1         # no units
M = 50                  #in M_sun
v_inf = 0.01*kmsec_U    #speed at infinity for singlet in code
                                    units
scalefactor = 5         # no units

pos_SMBH = np.array([0,0,0])
M_SMBH = 10**9

m0_arr  = M*np.ones(nr_obj, dtype='d')
m_bin    = 2*M

SMA_bin_tot = np.array([1e1])

TIDAL_SCALAR_tot = np.array([1e2])
Number_iter = 1


for q in range(len(TIDAL_SCALAR_tot)):
    if (SMBH_bool == True):
        result = np.zeros([len(SMA_bin_tot),Number_iter])
    for k in range(len(SMA_bin_tot)):
        if (SMBH_bool == False):
            result = np.zeros(Number_iter)
        SMA_bin = SMA_bin_tot[k]
        T_orb_bin = 2.*np.pi*np.sqrt((SMA_bin**3.)/(3*M))
        T_max = 100 * T_orb_bin

        if (SMBH_bool == True):
            R_t = TIDAL_SCALAR_tot[q]*SMA_bin*(M_SMBH/(3*M))**(1/3)
            V_t = np.sqrt((M_SMBH+3*M)/R_t)

            r_tidal = R_t*np.array([1,0,0])
            v_tidal = V_t*np.array([0,1,0])


        for j in trange(Number_iter):
            Y0  = np.zeros(nr_obj*6,    dtype='d')
```

```
Y0 = Init_condition(SMA_bin,m0_arr,Y0)


RVA_parameter = relativePVfunction(Y0)

dt_step = func_dt(RVA_parameter)
#choose dt:
dt_evolve   = dt_scale*dt_step

YY = solve_ivp(func_NBODY_Ydot,(0.0,T_max),Y0,method =
                                    'LSODA', atol=1e-6,
                                    rtol=1e-6, events = [
                                    SchwarzschildMerger,
                                    BodyMerger3,Ejection]
                                    )


Y_final2 = YY.y
t = YY.t


events = YY.y_events
# print(events)
lev = np.zeros(len(events))
for i in range(len(events)):
    lev[i] = len(events[i])

    if (SMBH_bool == True):
        result[k,j] = result[k,j] + (i+1)*lev[i]
    else:

        result[j] = result[j]+(i+1)*lev[i]
    # print(result)



if (SMBH_bool == True):
    result[k,j] = BodyMerger2(result[k,j],Y_final2)
    if result[k,j] == 3:
        RVA_parameter = relativePVfunction(Y_final2[:,-
                                           1])
        com_arg = np.where(RVA_parameter[2] ==
                                           RVA_parameter
                                           [2].min())
        T_GW = (c_SI**5/G_new_SI**3 * AU_SI**4 /
                                           M_sun_SI**3)/
                                           (sec_year) *
                                           merger_time(
                                           RVA_parameter
                                           ,m_bin,
                                           com_arg)
        # print(T_GW/10**5)
        if (T_GW < 10**5):
            # print('GW inspiral')
            result[k,j] = result[k,j]+1
else:
```

```
                result[j] = BodyMerger2(result[j],Y_final2)
                if result[j] == 3:
                    RVA_parameter = relativePVfunction(Y_final2[:,-
                                                       1])
                    com_arg = np.where(RVA_parameter[2] ==
                                                       RVA_parameter
                                                       [2].min())
                    T_GW = (c_SI**5/G_new_SI**3 * AU_SI**4 /
                                                       M_sun_SI**3)/
                                                       (sec_year) *
                                                       merger_time(
                                                       RVA_parameter
                                                       ,m_bin,
                                                       com_arg)
                    # print(T_GW/10**5)
                    if (T_GW < 10**5):
                        # print('GW inspiral')
                        result[j] = result[j]+1
```

References

[1] P. C. et al. Peters. "Gravitational Radation from Point Masses in Keplerian Orbit". In: *The Physical Review* (1963).

[2] M. Valtonen & H. Karttunen. *The Three-Body Problem*. Cambridge University Press, 2006.

[3] J. et al. Samsing. "The Formation of Eccentric Compact Binary Inspirals and the Role of Gravitational Wave Emission in Binary-Single Stellar Encounters". In: (2013).

[4] Marchant P. et al. "A new route towards merging massive black holes". In: (2016).

[5] L. Blanchet. "Gravitational Radiation from Post-Newtonian Sources and Inspiralling Compact Binaries". In: (2016).

[6] I. et al. Mandel. "Merging binary black holes formed through chemically homogeneous evolution in short-period stellar binaries". In: (2016).

[7] M. Celoria et. al. *Lecture notes on black hole binary astrophysics*. 2018.

[8] J. et al. Samsing. "Active Galactic Nuclei as Factories for Eccentric Black Hole Mergers". In: (2020).

[9] D. et al. Britt. "Binary black holes mergers from hierarchical triples in open clusters". In: (2021).

[10] B. et al. Liu. "Enhanced Black-Hole Mergers in Binary-Binary Interactions". In: (2021).

[11] Mapelli M. "Binary black hole mergers: formation and populations". In: (2021).

[12] H. et all Tagawa. "Formation and evolution of compact object binaries in AGN disks". In: (2021).